Solid Volume Calculator

An Approach to Glass Molds In-line Inspection

Gabriela Magalhães de Sousa

Thesis to obtain the Master of Science Degree in

Mechanical Engineering

Supervisors: Prof. Carlos Baptista Cardeira
Prof. Mário António da Silva Neves Ramalho

Examination Committee

Chairperson: Prof. Paulo Jorge Coelho Ramalho Oliveira
Supervisor: Prof. Mário António da Silva Neves Ramalho
Member of the Committee: Prof. Alexandra Bento Moutinho

October 2020

Acknowledgments

I would like to thank my supervisors Prof. Mário Ramalho and Prof. Carlos Cardeira for all the time and attention they spent.

Intermolde's cooperation made possible the use of real glass molds directly from the industry with the knowledge behind its production and they also made available scans of some molds by them requested to Microsense.

Thanks to Intermolde and its collaborators, in particular to Eng. Ricardo Ferreira , Dr. Sérgio Simões and Nélio Duarte. The knowledge and resources made available were crucial to the development of this master thesis.

The tests performed were possible thanks to the cooperation of *Laboratório de Biomecânica de Lisboa*, *Lab2Prod* and the resources available at *FabLab Lisboa*.

Also in what concerns hardware used in the tests carried out, ACCAII laboratory made available several materials such as the conveyor and the RGBD cameras. This project started as an assignment for the Curricular Unit of Mechatronic Systems, for that I thank the Faculty and my colleague Pedro Santos.

I would like to thank Prof. Miguel Tavares da Silva and Sérgio Gonçalves, from *Laboratório de Biomecânica de Lisboa*, and Prof. Relógio Ribeiro, Prof. Marco Leite and Manuel Sardinha, from *Laboratório para Desenvolvimento do Produto*, for their availability and for sharing their knowledge on scanners.
I also appreciate the help, kindness and suggestions of the collaborators of *FabLab Lisboa*.

A special thank you to my friends and lab mates that kept me motivated. To AEIST futsal team.

Last but not least, a big thank you to my parents Paula and Eduardo, my brother Guilherme and my cousin Joana.

Abstract

This dissertation consists in the study of the possibility of implementing a solution to perform quality inspection of molds' inner cavities for the glass mold industry.

The intended solution requires a series of specifications from the company that provided the problem that led to the exploration of 3D scanning commercial solutions as a tool to simplify and make the process of inspecting the molds faster to the operator.

Three approaches are proposed and explored, the first one working with simple geometric shapes that allow the identification along the part determining the parameters that define the shape, with this information the volume is analytically computed. The second method intends to go further and account for complex shapes and engravings in the mold, by going through each section iteratively, polynomials are fitted into the curves that will allow the computation of the volume of each cavity by means of integration. The last method presented took a step back and computes the volume based on the revolution of the profile of the mold.

For the first two methods tests were performed in simulation as well as with real data, while for the last one only real data tests were effected. Promising and consistent results were obtained that indicate the viability of the solution.

The third method goes far beyond volume computation itself, it illustrates the difficulties encountered during the search for a solution allowing to define unambiguously relevant parameters in what concerns specifications.

Considering the work developed, guidelines for further work are discussed.

Keywords: Volume, Molds, 3D Scanner, Metrology, Inspection, Quality.

Resumo

Esta dissertação consiste num estudo da possibilidade de implementação de uma solução para a inspeção de qualidade das cavidades interiores de moldes para a indústria vidreira.

A solução pretendida requer uma série de especificações definidas pela empresa que sugeriu o problema que fizeram com que se optasse por explorar soluções de scanners 3D comerciais de forma a simplificar e tornar mais rápido o processo para o operador.

Três propostas são exploradas, a primeira funciona com formas geométricas simples e permite identificar as mesmas ao longo da peça determinando os parâmetros que definem essa mesma forma e analiticamente calcula o volume. O segundo método pretende ir mais longe e ser capaz de lidar com formas complexas e gravações no molde, assim, percorrendo iterativamente cada secção do molde ajustam-se equações polinomiais que vão permitir determinar um volume de cada cavidade separadamente através de integração. A terceira proposta dá um passo atrás e através de revoluções de perfis de molde obtém um volume.

Para os dois primeiros métodos são realizados testes tanto em simulação como com dados reais, enquanto que para o último foram realizados testes apenas com dados reais. Apresentando-se resultados consistentes e promissores de que uma solução neste sentido será viável.

O terceiro método vai para além do cálculo de volumes, ilustra algumas dificuldades encontradas ao longo do desenvolvimento e permite definir inequivocamente parâmetros necessários no que toca às especificações.

De acordo com todo este trabalho discutem-se ainda linhas orientadores para trabalho futuro no sentido da melhoria das soluções propostas.

Palavras-Chave: Volume, Moldes, Scanner 3D, Metrologia, Inspeção, Qualidade.

Contents

List of Tables

List of Figures

Acronyms

fps frames per second. 33

ICP Iterative Closest Point. vii, 11, 23, 32, 35, 45, 50, 52, 58, 62

IR Infrared. 33

RANSAC Random Sample Consensus. vii, 16, 62

RGB Red Green and Blue. 5, 33, 35

RGBD Red, Green, Blue and Depth. 33, 37, 63

RMS Root Mean Square. 11

RMSE Root Mean Square Error. 25

ROI Region Of Interest. 37, 46, 56, 58

ToF Time of Flight. viii, 33

Chapter 1

Introduction

The purpose of this dissertation is to evaluate methods for measuring the volume of mold cavities. The glass mold industry is searching for a solution to test its production with precision and in a functional way, as in the production line it is not possible to ensure that no errors occur.

ISO 2859 standard defines inspection as "The process of measuring, examining, testing, gauging or otherwise comparing the unit of product with the applicable requirements"[6].

The unit of product is also defined in the same standard as being the "item inspected in order to determine its classification as conforming or nonconforming or to count the number of nonconformities. It may be a single article, a pair, a set, a length, an area, an operation or a volume"[6].

Quality control and inspection focus on guaranteeing the fulfillment of all requirements whether they are imposed by the customers or for technical reasons.

With the increase of the production, it is necessary to accelerate the process of inspecting, this is possible resorting to the automation of processes.

The need for quality inspection is required, according to the Industrial Partner, by the costumer as some of them require the volume of each mold individually.

For the company, the benefits of quality inspection do not represent directly a cost reduction as it is performed in the end of the production line, and at this point in most cases there is no chance of correcting previous errors.

The value in scope here is the volume rather than a specific length. So this procedure does not directly allow to find where the problem is located, it only detects the existence of a non-compliance with the tolerance. Although it can be extended if required.

Quality inspection will be performed mainly to fulfill costumers' requirements but also to ensure quality to new possible clients and as a feedback to the operators of the line. It will allow an understanding of the errors being generated and where in the production line they are occurring, allowing improvement.

Indirect improvement on the production can mean a cost reduction as nonconformity is expected to reduce once the problem in the production line is known and corrected.

The objective is to develop a general solution for volume inspection for industries, taking into account some specifications suggested by the company in the glass mold industry.

Several techniques were considered and studied in what concerns the data acquisition and processing as well as in terms of physical implementation solutions.

The approach to design and develop in this dissertation distinguishes itself from known applications since the volume to measure is a cavity and not the actual object. This implies different requirements and constraints to be further explored.

1.1 Quality Challenges

The problem arose at Intermolde, a Portuguese company based at Marinha Grande, a region internationally known for its glass industry.

This company accepts a wide-range of types of projects producing different forms and sizes of molds in several materials.

This will cause a high variability of tolerances and shapes to check.

Intermolde defines quality as "the set of specifications of a product/service that influences and determines our ability to fulfill and overcome the Costumers needs, demands and expectations." [7].

1.2 Mold Description

The scope is glass molds and their inner cavity. That is a complex surface, curved, defining the shape of the bottle with the particularity of being made of polished metal, making the surface extremely shinny. Thus, it is challenging to fit a geometric shape to the mold outline. Also shinny surfaces are very difficult to scan.

Dimensions of molds can vary depending on the bottle to produce, even for the same mold dimensions there are slight variations leading to different volumes.

A mold consists of three parts: two cavities, one male and one female, and the bottom part as shown in Figure 1.1. The material is either cast iron as shown in Figure 1.1a or bronze as shown in Figure 1.1b.

(a) Cast Iron Blow Mold   (b) Bronze Blow Mold

Figure 1.1: Examples of molds produced at the Industrial Partner
.

For the purpose of this project only the two cavities will be used since it was considered that bottom parts are not so concerning and susceptible to production errors. One relevant characteristic of parts is their curvature at the top. The apparent planes have in fact a curvature of approximately 0.1% of the total longitudinal length.

This feature will be studied along the development of a solution, as it is relevant to the total volume. It will be researched if it is precisely detectable and relevant.

1.3 Structure of the Dissertation

This document consists of 6 chapters:

The first chapter introduces the problem, by defining the goals and explaining the need that motivated this thesis.

The second chapter analyses the state of the problem, similar applications are researched, introductory considerations and the technological solutions to consider are discussed.

In the third chapter the methods and the underline theory used and considered in the several approaches are introduced. It also presents the algorithms for volume calculation used in the Implementation.

Chapter four concerns the implementation description, including both the technological and algorithmic solutions and its practical challenges. Several market solutions as well as professional/ industrial equipment are referred to. Four implementation approaches are described.

The fifth chapter presents the results of the several approaches using different scanning devices, hardware requirements are then stated.

Finally in the last chapter conclusions and results are discussed. Suggestion for further development of the subject are also presented in this section.

Chapter 2

State of the Art

The techniques and technologies already in place and approaches related to volume measuring allowed to acquire experience and learn advantages and disadvantages of each approach and where difficulties can arise from. Although few references are found in the subject it is not possible to determine *a priori* which will be the way forward towards the desired goal. Despite that, all of the mentioned before need to be taken into account developing a new concept or solution.

Also research in in apparently unrelated areas can provide valuable information. Therefore state of the art research and commercial solutions are discussed in this chapter by means of a bibliographic review.

2.1 Solid Volume Measuring Solutions

The first method studied focuses on finding the inliers of the planes of a scene and, subsequently, the vertices that connect adjacent planes of the object, so that it is possible to determine each edge length.

The system work flow proposed in [1] is presented in the Figure 2.1, illustrating the high-level operation of the application and as shown in Figures 2.2 and 2.3.
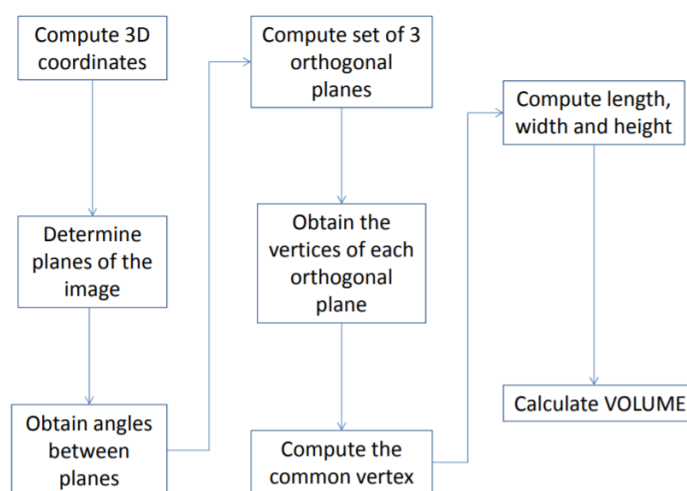
Figure 2.1: Workflow of the system proposed in [1]

In [1] the tests are performed with a box, both Red Green and Blue (RGB) and depth images are acquired from the cameras and the depth information is used to compute the 3D coordinates (X, Y, Z),

using the camera model to obtain a 3D point cloud representation. Invalid point readings caused by points out of range or lighting conditions are removed from the set.

Having classified all points as either inliers or outliers, the two planes with most inliers are removed. This can also be performed by background subtraction [1]. Afterward the angle between each pair of neighboring planes is computed to determine the right edges relevant for the volume computation. The planes are projected into a 2D binary image and morphological operations are applied to overcome missing data and to be able to use Harris corner detector, according to [1].
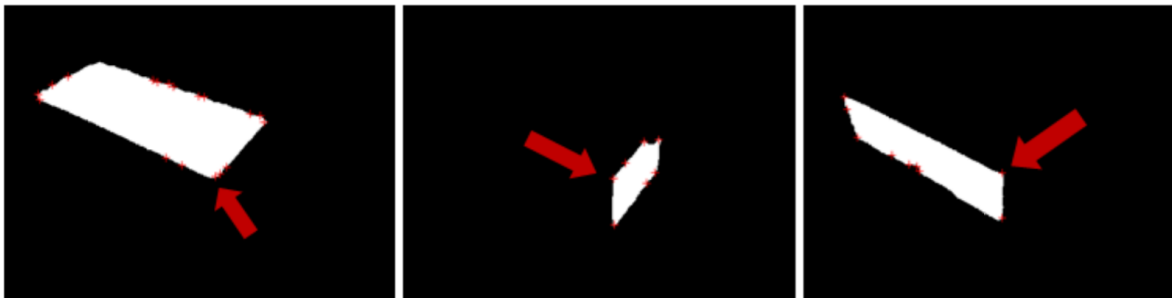
Figure 2.2: Detected corners and the vertex common to the three orthogonal planes pointed out with an arrow. Source: [1]

The key phase when dealing with the corner detection is to choose the common vertex, then by using euclidean distance the edges length is computed allowing the volume to be computed as well.
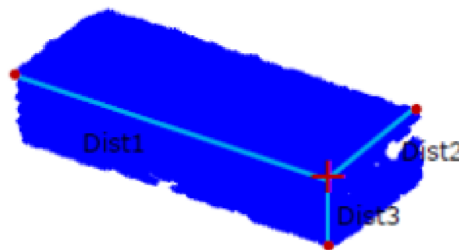
Figure 2.3: Common vertex and the vertices used to compute the length of the three edges. Source:[1]

It was decided to implement this method with higher resolution cameras as a learning process and a test to cameras that were considered for point cloud acquisition.

Although research for internal volume is scarce there are approaches in other fields that may be adapted for the mold volume measuring in particular. In [8] an algorithm to measure tree volume is developed. In [9] a solution is proposed for waste volume calculation to monitor the capacity of the landfill.

In [10] it is suggested the Slicing Algorithm for point clouds for rapid prototyping.

Based on [8], [9] and [10], a method for volume computation was created and tested in [11].

The tests are performed in simulation only and without the presence of noise. In [11] the process begins by loading the point cloud, slices it and saves them for post processing. Slices are then cut into smaller groups of close points and those points are also saved to each of these last groups of points the fit a curve of an order calculated based on the number of inflection points.

The method described in [11] differs from the one proposed in the shapes as it is intended to simulate

actual molds and compute their real volume, it differs in the method of fitting a curve as the slices will not be sub-sampled.

One should also be critical in what concerns the results presented in table I on [11] as the true volumes are not in the same range thus creating the possibility of a false tendency in the percentage error.

2.2 Current Procedures in the Mold Industry

2.2.1 Mold Filling

The task is currently performed by an operator, the mold is joined filling the gaps with an appropriate paste. Having the mold closed it is filled with water, determine the mass of water and its temperature in order to theoretically determine the water density using tables.

The accuracy of this method considering the uncertainty of the whole process is $\pm0,1ml$ for molds with volume of approximately 100ml and $\pm0,25ml$ for molds with volume around 1000ml.

There is an error associated with cohesion, a key property of water that measures how well molecules stick to each other or group together. A strong Coulomb attraction between the molecules draws them together due to the capacity of water molecule to form four hydrogen bonds with neighboring molecules. As water molecules are more strongly attracted to each other than to other molecules, they form a dome when filling a container before spilling over the sides [12].

This error is completely dependent of the operator sensibility and experience and for this reason it is not completely measurable. The uncertainty claimed by the Industrial Partner requires an experienced operator, since it is considered adequate these measures are going to be used as a reference to real molds when necessary.

Although the time to take the measure of a single mold is around 10 min according to the Industrial Partner, it is required to close every single mold and to clean it after the test as the past sticks to the part, this represents a relevant amount of the of the test's time.

2.2.2 Sonicam S3

Another method to measure molds inner volume is Sonicam S3 [13]. It is a system shown in Figure 2.4 designed to fill a balloon, called a bladder, as it can be seen in Figure 2.4b. Bladders are produced by the same supplier of the device in several sizes specific to each type of mold and range of volumes to measure or with the desired dimensions in case of a special order if it fits the minimum and maximum dimensions described in the technical specifications [13]. It performs automatic correction of temperature.

Although this device produces results in a time interval considered reasonable, the result is by comparison and does not give information about where the defect is located. Additionally corners and high variation details do represent potential for increasing of the error. Also the machine has a cost considered high for small industries, it spends consumables and requires costly maintenance.

Sonicam S3's measures [13] have an uncertainty of $\pm0.05ml$ for molds of around 100ml and $\pm0.09ml$ for molds with approximately 1000ml.

The device has limitations in what concerns the maximum volume, some diameters of the mold as well as its height, this implies that S3 can't be used for the all types of molds produced.

7

(a) Machine   (b) Detail of the bladder in the mold

Figure 2.4: Sonicam S3 - Mold Gauging Machine

2.3 Problem Statement

Molds' inner cavities have complex shapes and engravings as illustrated by Figures 2.5 and 5.7 and the series are short, 12 to 90 units [7], with a typical value being 30 molds. This means that the molds to inspect are very different from each other, thus a generalized method is desired.

To illustrate the range of values that engravings account for, the center engraving, the number and the line bellow it represent less than $0,1ml$, which is half of the uncertainty of the method currently used by the Industrial Partner.

Figure 2.5: Example of engravings that can be present in bottle molds - Bottom part of Ref.9158

It is important to understand the complexity of the molds produced for the glass industry in order to develop an effective solution.

As an example, one can observe the technical drawing of a blank mold, one of the less complex ones,

8

in Figure 2.6 (a). Also a more complex finishing mold is presented in 2.6 (b), to note that in the drawing two engraving sections with logos and technical markings are not represented but add complexity to it.

(a) Ref. 11937 - Blank Mold

(b) Ref. 0561 - Beer bottle mold
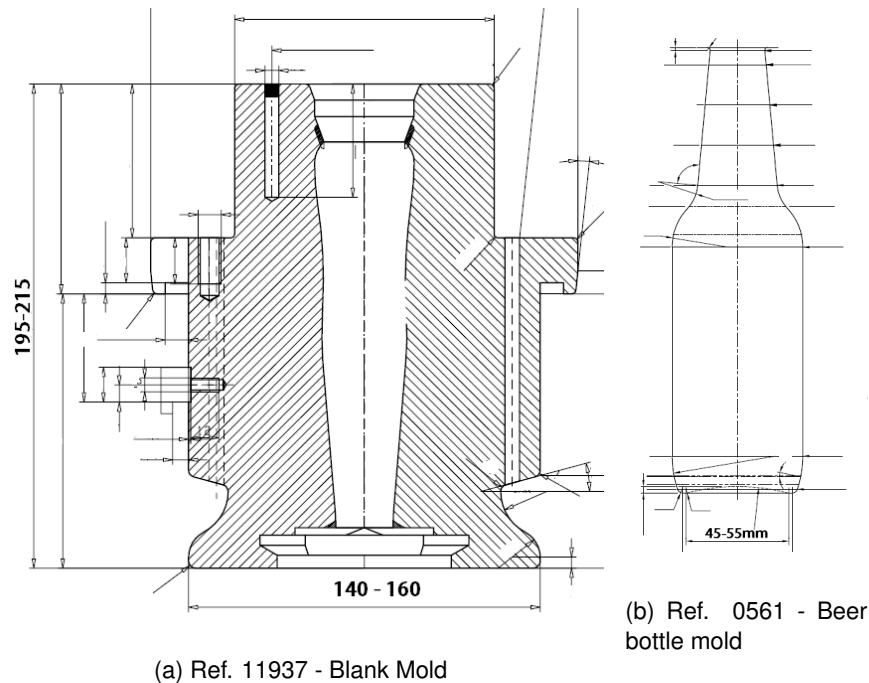
Figure 2.6: Technical Drawing of two molds

Only typical dimensions range is indicated for visualization in Figures 2.6.

Both the materials presented are very bright and reflective, presenting a diffuse reflection as it is possible to observe in Figure 2.7.

Another relevant fact in a production line of the mold glass industry is that each bottle mold is produced almost to the end until the next mold enters the line. This means the machine tool wears out, for instance, when one part is being machined, allowing the possibility of the next part having dimensional variations, these variations have to be assessed in order to determine if they are inside or outside the allowed tolerance.

All these factors justify the need of inspecting every mold and in every section of the mold, thus it is undesirable to extrapolate missing data.

According to the Industrial Partner's requirements the method to develop is intended to be a solution with the following characteristics:

- The inspection can't be destructive or somehow damage the part, scratches on the surfaces can lead to and accelerate undesired oxidation;

- Use commercial scanning solutions;

- No surface aids are allowed, such as powders or sprays to overcome issues caused by brightness;

- No stickers with glue such as targets to overcome alignment problems caused by symmetries in the part can be used;

- The solution must be fast enough to be applied in-line, the time indicated by the Industrial Partner is around 20 minutes, but this depends on the type of mold and its production time.

The usage of stickers, powders or sprays would not decrease task time. As molds have to be delivered clean, as it would be a risk to clog the narrow pores existing in the part, cleaning time should be accounted.

9

Figure 2.7: Example of engravings and light diffuse reflection in a bronze mold - Ref. 2283 female

Chapter 3

Methods

Several approaches are possible. This chapter presents and assess the usefulness of several mathematical tools to be developed in the implementation phase in order to converge to a method of obtaining the volume of solids from simple to complex shapes and in particular mold cavities.

3.1 ICP and its relevance

Iterative Closest Point (ICP) is an algorithm to register two point clouds resulting in a transformation matrix that minimizes the distance between each source point to its match, as illustrated in Figure 3.1 where the cloud b) is registered to a) resulting in d). It is widely used in aligning three dimensional models given an initial guess of the rigid body transformation which is our main interest but may also be used to localize robots or to achieve optimal path planning according to [2].

This method has the capability to align clouds acquired by different cameras or by the same camera given different points of view. It has its better application when the clouds to align are not symmetric and have features to allow a fast convergence of the fitting.

Almost all 3D Scanners' software use this method to align several views from the same sensors although this fails when there's symmetry of the parts as there are multiple solutions. This is solved in general by scanners producers by adding targets in the part, stickers with a specific shape and color to add features. When this is not possible the software requires 3 pairs of matching points for a first transformation matrix guess.

Other solutions can be applied to solve this issue, for example by adding background features in the acquisition and then subtracting them in the pre-processing phase.

3.1.1 Iterative Closest Point Algorithm

The Iterative Closest Point treats correspondence as a variable to be estimated [14]. The inputs to this algorithm are the reference and the source point clouds, an initial estimation of the transformation (or a random one) and also stopping criteria. The output is a refined transformation.

The algorithm consists in matching the closest point from a selected set in the reference point cloud for each point in the set of each model. Then it estimates the combination of rotation and translation using Root Mean Square (RMS) point to point distance minimization technique, this aligns each source point to its match. The transformation is applied and the algorithm iterated saving the best solution so far.

The method is briefly summarized in Figure 3.2.
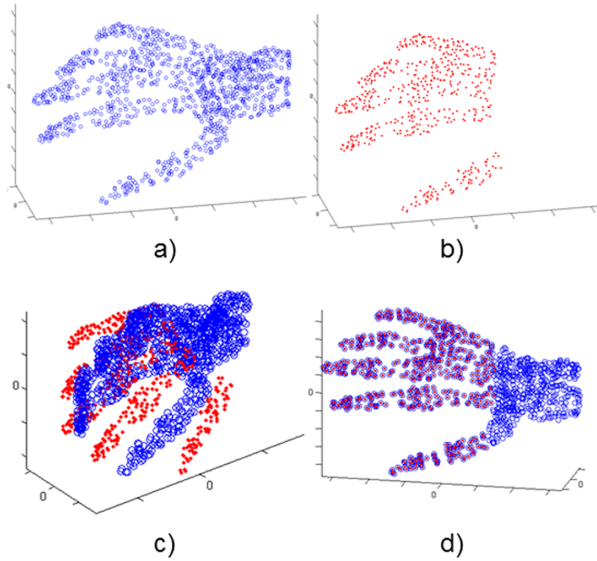
Figure 3.1: Example of ICP application [2]
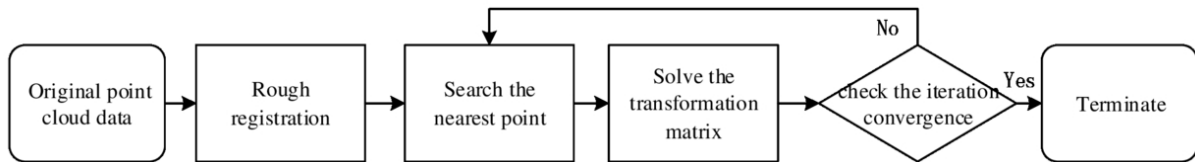
Figure 3.2: ICP Algorithm

3.2 The Least Squares Criteria

The estimation method to be used in our approach is algebraic and based on the least squares method in order to obtain a parametric fitting of the curves that are part of the mold. With this method it is expected to obtain a very accurate measure of the volume of these molds, as defined in the specifications.

The least squares method is a criteria to find the best-fitting curve to a given set of points by minimizing the sum of the squares of the offsets, the so called "residuals" of the points from the curve.

The sum of the squares of the offsets is used instead of the offset absolute values because this allows the residuals to be treated as a continuous differentiable quantity.

3.2.1 2D Least Squares

Consider the equation that defines a line in the xy plane represented in figure 3.3:

$$y = mx + b \tag{3.1}$$

$$\begin{cases} \overline{y}_1 - mx_1 - b \\ ... \\ \overline{y}_i - mx_i - b \end{cases} \tag{3.2}$$

Defining J as the cost function:
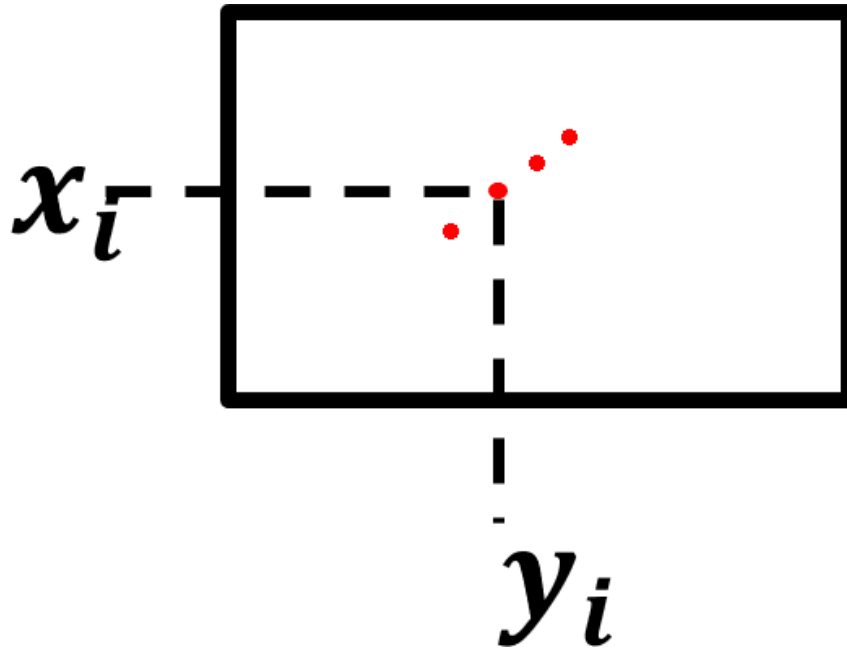
Figure 3.3: Representation of data points in the plane

$$J = \left(\begin{array}{c} \overline{y}_1 - \begin{bmatrix} x_1 & 1 \end{bmatrix} \begin{bmatrix} m \\ b \end{bmatrix} \\ ... \\ \overline{y}_m - \begin{bmatrix} x_m & 1 \end{bmatrix} \begin{bmatrix} m \\ b \end{bmatrix} \end{array} \right)^2 \tag{3.3}$$

Expanding function J:

$$J = \left(\begin{bmatrix} \overline{y}_1 \\ ... \\ \overline{y}_m \end{bmatrix} - \begin{bmatrix} x_1 & 1 \\ ... & ... \\ x_m & 1 \end{bmatrix} \begin{bmatrix} m \\ b \end{bmatrix} \right)^T \left(\begin{bmatrix} \overline{y}_1 \\ ... \\ \overline{y}_m \end{bmatrix} - \begin{bmatrix} x_1 & 1 \\ ... & ... \\ x_m & 1 \end{bmatrix} \begin{bmatrix} m \\ b \end{bmatrix} \right) \tag{3.4}$$

For simplicity's sake the matrices will hereinafter be referred to in the form of:

$$\overline{Y} = \begin{bmatrix} \overline{y}_1 \\ ... \\ \overline{y}_m \end{bmatrix} \tag{3.5}$$

$$A = \begin{bmatrix} x_1 & 1 \\ ... & ... \\ x_m & 1 \end{bmatrix} \tag{3.6}$$

$$X = \begin{bmatrix} m \\ b \end{bmatrix} \tag{3.7}$$

Continuing by minimizing the cost function:

$$minJ = min \left(\overline{Y} - AX \right)^T \left(\overline{Z} - AX \right) \tag{3.8}$$

$$minJ = min\left(\overline{Y}^T - X^T A^T\right)^T \left(\overline{Y} - AX\right) \tag{3.9}$$

$$minJ = min\left(\overline{Y}^T\overline{Y} - X^T A^T\overline{Y} - \overline{Y}^T AX + X^T A^T AX\right) \tag{3.10}$$

Let's now minimize the cost function by setting the derivative in respect to X (the vector of coefficients of the parameterization) equal to zero:

$$\frac{\partial}{\partial X}J = \left(-2A^T\overline{Y} + 2A^T AX\right) = 0 \tag{3.11}$$

$$2A^T AX = 2A^T\overline{Y} \tag{3.12}$$

$$X = \left(A^T A\right)^{-1} A^T\overline{Y} = \begin{bmatrix} m \\ b \end{bmatrix} \tag{3.13}$$

3.2.2 3D Least Squares

To illustrate the least squares approximation in 3D let us a consider the parameterization of a generic plane in the 3D space in Cartesian coordinates as represented in Figure 3.4:

$$z = ax + by + c \tag{3.14}$$

This can be interpreted as each point in the 2 dimensional space as associated a z coordinate corre-
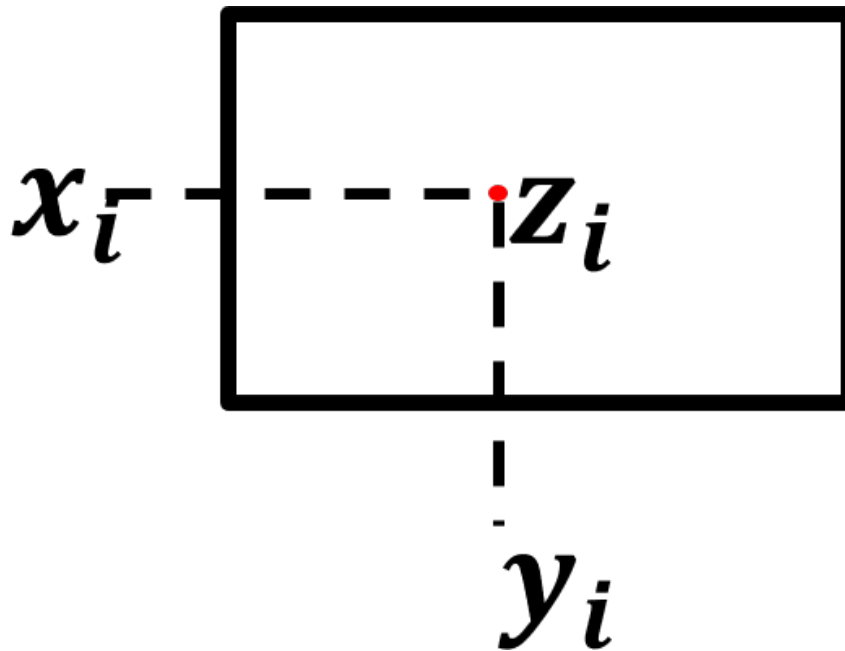
Figure 3.4: Representation of a point in space

sponding to the depth.

The objective is now having a point cloud, obtained with some camera or simulated data, adjust it to the parametric equation, z represented with an over line corresponds the points from the point cloud while z belongs to the parameterization. The difference is that the point cloud is affected by noise or errors in the imperfections found in the produced geometry. These interference will be studied in a further section.

So the error between the point cloud z and the values from the parametrerization are given by the

set:

$$\begin{cases} \overline{z}_1 - ax_1 - by_1 - c \\ ... \\ \overline{z}_i - ax_i - by_i - c \\ ... \\ \overline{z}_m - ax_m - by_m - c \end{cases} \tag{3.15}$$

Defining a cost function J as the square error for each point:

$$J = \begin{pmatrix} \overline{z}_1 - \begin{bmatrix} x_1 & y_1 & 1 \end{bmatrix} \begin{bmatrix} a \\ b \\ c \end{bmatrix} \\ ... \\ \overline{z}_m - \begin{bmatrix} x_m & y_m & 1 \end{bmatrix} \begin{bmatrix} a \\ b \\ c \end{bmatrix} \end{pmatrix}^2 \tag{3.16}$$

Expanding the function J:

$$J = \left(\begin{bmatrix} \overline{z}_1 \\ ... \\ \overline{z}_m \end{bmatrix} - \begin{bmatrix} x_1 & y_1 & 1 \\ ... & ... & ... \\ x_m & y_m & 1 \end{bmatrix} \begin{bmatrix} a \\ b \\ c \end{bmatrix} \right)^T \left(\begin{bmatrix} \overline{z}_1 \\ ... \\ \overline{z}_m \end{bmatrix} - \begin{bmatrix} x_1 & y_1 & 1 \\ ... & ... & ... \\ x_m & y_m & 1 \end{bmatrix} \begin{bmatrix} a \\ b \\ c \end{bmatrix} \right) \tag{3.17}$$

For simplicity the matrices will hereinafter be referred to in the form of:

$$\overline{Z} = \begin{bmatrix} \overline{z}_1 \\ ... \\ \overline{z}_m \end{bmatrix} \tag{3.18}$$

$$A = \begin{bmatrix} x_1 & y_1 & 1 \\ ... & ... & ... \\ x_m & y_m & 1 \end{bmatrix} \tag{3.19}$$

$$X = \begin{bmatrix} a \\ b \\ c \end{bmatrix} \tag{3.20}$$

Continuing by minimizing the cost function:

$$minJ = min \left(\overline{Z} - AX \right)^T \left(\overline{Z} - AX \right) \tag{3.21}$$

$$minJ = min \left(\overline{Z}^T - X^T A^T \right)^T \left(\overline{Z} - AX \right) \tag{3.22}$$

$$minJ = min \left(\overline{Z}^T \overline{Z} - X^T A^T \overline{Z} - \overline{Z}^T AX + X^T A^T AX \right) \tag{3.23}$$

Now minimizing the cost function by setting the derivative in respect to X (the vector of coefficients of the parameterization) equal to zero:

$$\frac{\partial}{\partial X} J = \left(-2A^T \overline{Z} + 2A^T AX \right) = 0 \tag{3.24}$$

$$2A^T AX = 2A^T \overline{Z} \tag{3.25}$$

$$X = \left(A^T A\right)^{-1} A^T \overline{Z} = \begin{bmatrix} a \\ b \\ c \end{bmatrix} \tag{3.26}$$

This method can be used to geometries other than a plane although the complexity of the computation is similar.

Another approach is the Random Sample Consensus Algorithm (RANSAC), as it is stated it is of particular interest combined with other estimation methods.

3.3   Outlier Rejection using RANSAC

The Random Sample Consensus Algorithm (RANSAC) is an iterative method that is used to estimate parameters of a mathematical model from a set of data containing outliers. The RANSAC algorithm assumes that all of the data is has both inliers and outliers [3].
Inliers can be described by a model with a particular set of parameter values, while outliers do not fit that model.
The input to the RANSAC algorithm is a parameterized model which can described or fitted to the observations with some reliability.

3.3.1   Random Sample Consensus Algorithm

This algorithm achieves its goal by iteratively selecting a random subset of the data which will be the hypothetical inliers and this hypothesis is then tested in the following sequence [3] :
Firstly a model is fitted to the hypothetical inliers, all the free parameters of the model are reconstructed from the inliers.
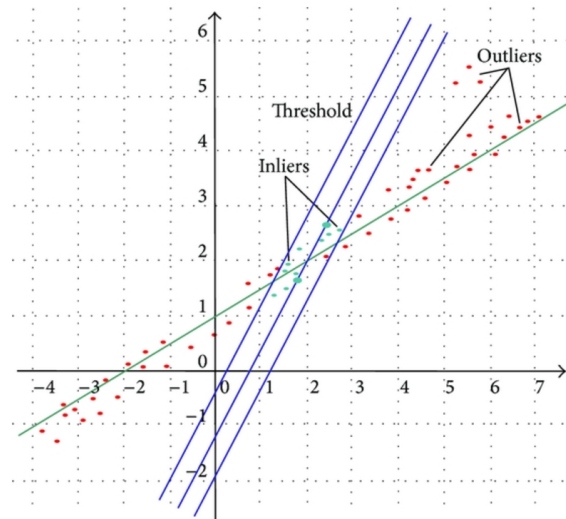
Figure 3.5: Illustration of the inliers and outliers classification with respect to random set with a given threshold [3]

Then all other data is tested against the fitted model. If a point fits the estimated model it is also considered as a hypothetical inlier.
The estimated model should now be considered reasonable or not, it is reasonably good if there is a sufficient amount of points classified as hypothetical inliers. The model is then re-estimated for the

hypothetical inliers, without the influence of the possible outliers, and it is evaluated by comparing it to the model.

The example in Figure 3.5 shows a random initial guess to the parameters and an illustration of an iteration in which the model is not reasonable as most of the data points are outliers thus the model is not representing the data.

All this procedure is iterated, meaning it is repeated a fixed number of times and at each iteration a new model is produced, it can either be rejected or not. If the model has an acceptable number of inliers and it has the lower error so far it is saved and the last saved model is deleted. If not enough points are considered inliers or if the model is worse in terms of error than the last one saved it is rejected and the procedure continues with the same best result as in the iteration before, meaning the lowest error result is the one kept.
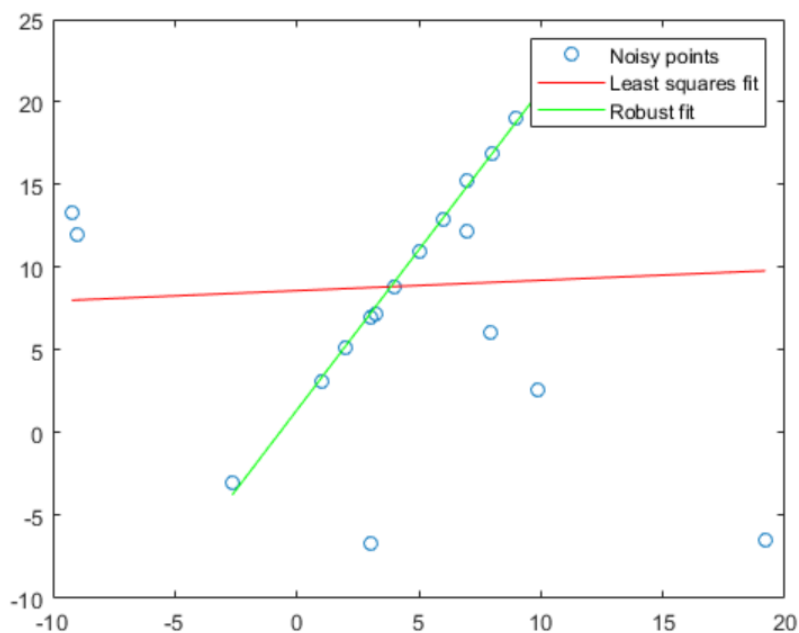
Figure 3.6: Matlab example of a comparison between the fit with the least squares per si and using RANSAC combined in the least squares (Robust Fit)

The difference in the accuracy of the methods is illustrated in Figure 3.6. As the Robust Fit method excludes the outliers from the data set used in the computations the error is clearly reduced.

For all these reasons this is a method to take into consideration in the image processing phase of this project and it will be implemented using Matlab's Computer Vision Toolbox.

3.4 Estimation Architecture

This Algorithm was developed to include three phases: the data acquisition, the pre-processing and the actual volume computation.

For the volume computation four solutions were developed. The first one designed to measure the volume of boxes, the second to measure volume of geometric shapes with a known model. The remaining two were designed specifically for molds even though they can have different applications, one assumes the mold is a revolution of a profile and thus circular, the last solution is a general solution in which the model is completely unknown and it is intended to work for any kind of mold produced.

3.4.1 Data Acquisition

The success and quality relies mainly in the quality of the input data, so in this phase it is important to choose an appropriate scanner as described in the technical solution available for the conditions of the room, for the material of the part to scan and concerning the budget of the intended application.

In this phase it is important to know the limitations such as precision and accuracy of the used scanner in order to define the error that may be caused by it.

The importance of the data obtained justifies the need to characterize parametrically the features in scope. This way it is possible to identify the differences between the acquisition and the object through a mathematical model. As is it demonstrated further the quality of the first cameras used show apparent insufficient results. Figures 3.10 and 5.5 allow us to compare the point cloud created with a mathematical model of the shape and the one acquired with an Intel Realsense camera.

3.4.2 Pre-processing

The pre-processing phase will consist in the selection of a region of interest where the cavity and the closing plane are located, in this phase lateral parts of the mold should be removed from the cloud, background is removed and there is also the possibility to include a method of removing noise.

This phase can be performed in most of the scanning device's software. It will be relevant to automate it when developing applications with technological solutions without its own software.

3.4.3 Box Volume Calculator

The first method tested was similar to the one proposed in [1] with some simplifications.

The simplification can be briefly described. A point cloud of the floor is taken for calibration as in Figure 4.10a and the equation of the floor plane is computed. Then for each box to measure a top view point cloud is acquired, as exemplified in Figure 4.10b.

The geometric center of the top plane is computed, knowing the center point (marked with letter "o" in Figure 3.7) the most distant point in the plane to the center will be assumed as one of the corners (marked with the letter C on Figure 3.7).
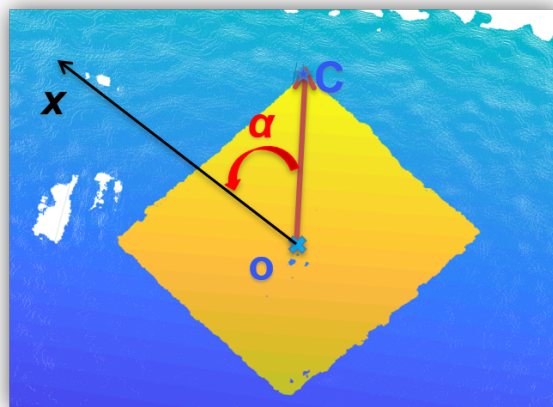
Figure 3.7: Schematic representation of the method to find the first corner C

The point cloud is rotated an angle α in z, such that the vector $\vec{oC}$ is aligned with the x axis. With this rotation, corners do now correspond to the maximum and minimum points in each direction as shown in Figure 3.8.
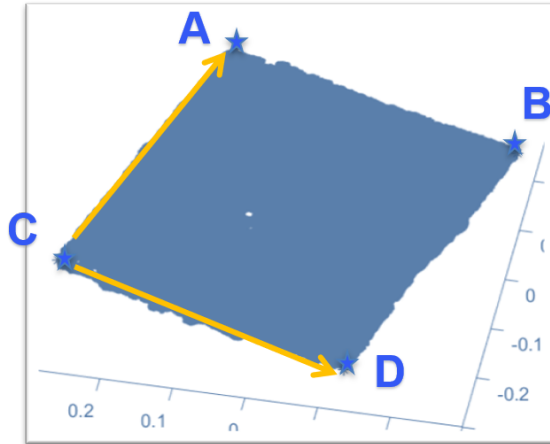
Figure 3.8: Schematic representation of the method to find the remaining corners
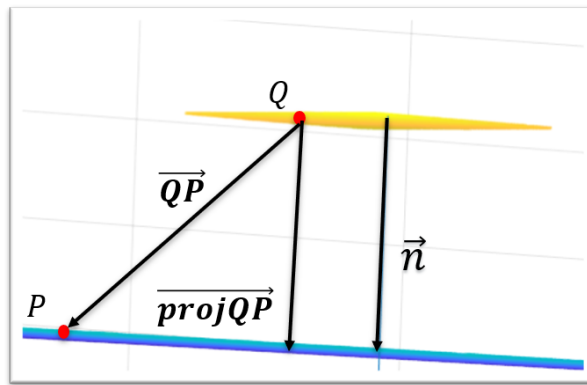
Figure 3.9: Schematic representation of the relevant vector

The dimensions of the box can now be determined by norms of vectors represented in Figures 3.8 and 3.9 using Equations 3.27 to 3.31.

$$Width = ||\overrightarrow{CD}|| \tag{3.27}$$

$$Depth = ||\overrightarrow{CA}|| \tag{3.28}$$

$$TOPArea = ||\overrightarrow{CA} \times \overrightarrow{CD}|| \tag{3.29}$$

$$\overrightarrow{projQP} = \frac{\overrightarrow{QP} \cdot \overrightarrow{n}}{||\overrightarrow{n}||^2} \tag{3.30}$$

$$Height = ||\overrightarrow{projQP}|| \tag{3.31}$$

The next section presents the Feature Recognition Approach, developed to compute simple solids' volumes by identifying and separating a wider problem in smaller ones that can be solved with known mathematical equations.

3.4.4 Feature Recognition Approach

The method implies total knowledge of the 3D shapes to be evaluated and its sequence through the longitudinal axis, although none of its dimensions needs to be known.

The principle is to segment each geometric form along the longitudinal axis by fitting the 3D shapes by the predefined order and determine the best fit of shapes that reduces the error when the parameters are computed by the Least Squares Method for 3D Shapes.
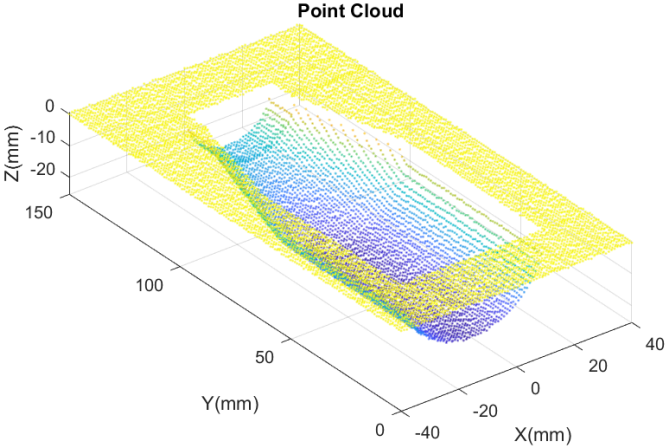
Figure 3.10: Generated Point Cloud

In Figures 3.11 and 3.12 one can observe the identification of the two cylinders in the point cloud in Figure 3.10 whose parameters are to be computed by the least squares method (colors and lines are represented for clarity).
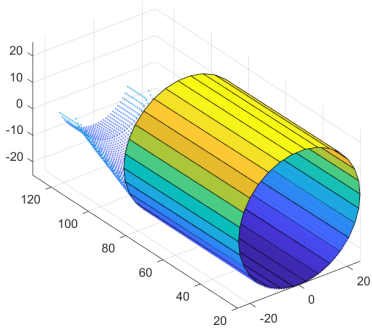
Figure 3.11: Segmentation of the first cylinder in the longitudinal axis
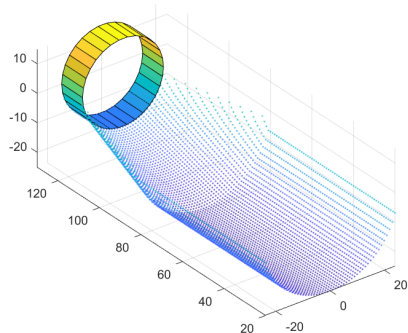
Figure 3.12: Segmentation of the second cylinder in the longitudinal axis

Parameter Calculation - The Least Squares Approach

The parameter calculation is done by the least squares criteria and it is implemented in matlab for the simple shapes as cylinders, spheres and ellipsoids.

This method was described in the sub section "Estimation Architecture" 3.4 for a general plane. In this section it is done for some of the simple geometries previously introduced and following the methodology explained in the Estimation Architecture 3.4.

Cylinder

The cylinder surface is defined by the equation:

$$x^2 + z^2 = r^2 \qquad (3.32)$$

So the error between each point in cloud z and the values from the parametrization are given by the set:

$$\begin{cases} \overline{z}_1^2 + {x_1}^2 - r^2 \\ ... \\ \overline{z}_i^2 + x_i^2 - r^2 \\ ... \\ \overline{z}_m^2 + x_m^2 - r^2 \end{cases} \qquad (3.33)$$

defining a cost function J as the square error for each point:

$$J = \begin{pmatrix} \overline{z}_1^2 - \begin{bmatrix} x_1^2 & -1 \end{bmatrix} \begin{bmatrix} 1 \\ r^2 \end{bmatrix} \\ ... \\ \overline{z}_m - \begin{bmatrix} x_m^2 & -1 \end{bmatrix} \begin{bmatrix} 1 \\ r^2 \end{bmatrix} \end{pmatrix}^2 \qquad (3.34)$$

Expanding the function J:

$$J = \left(\begin{bmatrix} \overline{z}_1 \\ ... \\ \overline{z}_m^2 \end{bmatrix} - \begin{bmatrix} x_1^2 & -1 \\ ... & ... \\ x_m^2 & -1 \end{bmatrix} \begin{bmatrix} 1 \\ r^2 \end{bmatrix} \right)^T \left(\begin{bmatrix} \overline{z}_1^2 \\ ... \\ \overline{z}_m^2 \end{bmatrix} - \begin{bmatrix} x_1^2 & -1 \\ ... & ... \\ x_m^2 & -1 \end{bmatrix} \begin{bmatrix} 1 \\ r^2 \end{bmatrix} \right) \qquad (3.35)$$

For simplicity the matrices will hereinafter be referred to in the form of:

$$\overline{Z} = \begin{bmatrix} \overline{z}_1^2 \\ ... \\ \overline{z}_m^2 \end{bmatrix}$$

$$A = \begin{bmatrix} x_1^2 & -1 \\ ... & ... \\ x_m^2 & -1 \end{bmatrix}$$

$$X = \begin{bmatrix} 1 \\ r^2 \end{bmatrix}$$

Continuing by minimizing the cost function:

$$minJ = min \left(\overline{Z} - AX \right)^T \left(\overline{Z} - AX \right) \qquad (3.36)$$

$$minJ = min \left(\overline{Z}^T - X^T A^T \right)^T \left(\overline{Z} - AX \right) \qquad (3.37)$$

$$minJ = min \left(\overline{Z}^T \overline{Z} - X^T A^T \overline{Z} - \overline{Z}^T AX + X^T A^T AX \right) \qquad (3.38)$$

Minimizing the cost function by setting the derivative in respect to X (the vector of coefficients of the

parameterization) equal to zero:

$$\frac{\partial}{\partial X} J = \left(-2A^T\overline{Z} + 2A^T A X\right) = 0 \tag{3.39}$$

$$2A^T A X = 2A^T \overline{Z} \tag{3.40}$$

$$X = \left(A^T A\right)^{-1} A^T \overline{Z} = \begin{bmatrix} 1 \\ r^2 \end{bmatrix} \tag{3.41}$$

Sphere

The sphere surface is defined by the equation:

$$x^2 + y^2 + z^2 = r^2 \tag{3.42}$$

So the error between each point in cloud z and the values from the parametrerization are given by the set:

$$\begin{cases} \overline{z}_1^2 + x_1{}^2 + y_1{}^2 - r^2 \\ ... \\ \overline{z}_i^2 + x_i{}^2 + y_i{}^2 - r^2 \\ ... \\ \overline{z}_m^2 + x_m{}^2 + y_m{}^2 - r^2 \end{cases} \tag{3.43}$$

Defining a cost function J as the square error for each point:

$$J = \left(\begin{matrix} \overline{z}_1^2 - \begin{bmatrix} x_1^2 & y_1^2 & -1 \end{bmatrix} \begin{bmatrix} 1 \\ 1 \\ r^2 \end{bmatrix} \\ ... \\ \overline{z}_m^2 - \begin{bmatrix} x_m^2 & y_m^2 & -1 \end{bmatrix} \begin{bmatrix} 1 \\ 1 \\ r^2 \end{bmatrix} \end{matrix} \right)^2 \tag{3.44}$$

Expanding the function J:

$$J = \left(\begin{bmatrix} \overline{z}_1 \\ ... \\ \overline{z}_m^2 \end{bmatrix} - \begin{bmatrix} x_1^2 & y_1^2 & -1 \\ ... & ... & ... \\ x_m^2 & y_m^2 & -1 \end{bmatrix} \begin{bmatrix} 1 \\ 1 \\ r^2 \end{bmatrix} \right)^T \left(\begin{bmatrix} \overline{z}_1^2 \\ ... \\ \overline{z}_m^2 \end{bmatrix} - \begin{bmatrix} x_1^2 & y_1^2 & -1 \\ ... & ... & ... \\ x_m^2 & y_m^2 & -1 \end{bmatrix} \begin{bmatrix} 1 \\ 1 \\ r^2 \end{bmatrix} \right) \tag{3.45}$$

For simplicity the matrices will hereinafter be referred to in the form of:

$$\overline{Z} = \begin{bmatrix} \overline{z}_1^2 \\ ... \\ \overline{z}_m^2 \end{bmatrix}$$

$$A = \begin{bmatrix} x_1^2 & y_1^2 & -1 \\ ... & ... & ... \\ x_m^2 & y_m^2 & -1 \end{bmatrix}$$

$$X = \begin{bmatrix} 1 \\ 1 \\ r^2 \end{bmatrix}$$

Continuing by minimizing the cost function:

$$minJ = min \left(\overline{Z} - AX \right)^T \left(\overline{Z} - AX \right) \tag{3.46}$$

$$minJ = min \left(\overline{Z}^T - X^T A^T \right)^T \left(\overline{Z} - AX \right) \tag{3.47}$$

$$minJ = min \left(\overline{Z}^T \overline{Z} - X^T A^T \overline{Z} - \overline{Z}^T AX + X^T A^T AX \right) \tag{3.48}$$

Minimizing the cost function by setting the derivative in respect to X (the vector of coefficients of the parameterization) equal to zero:

$$\frac{\partial}{\partial X} J = \left(-2A^T \overline{Z} + 2A^T AX \right) = 0 \tag{3.49}$$

$$2A^T AX = 2A^T \overline{Z} \tag{3.50}$$

$$X = \left(A^T A \right)^{-1} A^T \overline{Z} = \begin{bmatrix} 1 \\ 1 \\ r^2 \end{bmatrix} \tag{3.51}$$

The equations and parameters of the cone are obtained in a similar way, thus they are not presented.

The volume is determined by the parameters that define the solids. Consequently there are limitations to this method, it will only be possible to precisely determine the volume of solids with known equations.

In the glass mold industry blank molds are the ones that better fit this description as they are produced in larger series and commonly have simpler shapes. Even though the features in this type of molds are simpler there is not an analytic way to define them thus approximations are required, introducing potential errors off the desired tolerance.

The method implies, even for simple shapes, to have some sort of data base if it needs to implemented in the industry, where it could have its best application for objects with simple shapes and produced in larger series, such as packing boxes. This would allow easy identification of a nonconformity.

3.4.5 The Profile Revolution Approach

Considering the difficulties faced in the two methods presented before, a novel approach was developed to overcome the need of a known model for the features in a mold.

The Profile Revolution intends to meet the specifications in terms of time by taking the assumption that mold shapes are the revolution of a profile. This implies that only the profile will be taken into account. In this method, the remaining internal surface will not be considered.

The method begins by registering the top plane of the mold using ICP. The top plane is rotated and aligned with the x,y plane. The profile lines in each side of the cavity are identified, allowing to compute the distance between them. In the case of a cylindrical shape this distance corresponds to its diameter.

Infinitesimal volumes are computed and summed to obtain a total volume. The operator has to select manually the limits of the cavity's region of interest, since no general criteria was reached.

The application of this method is shown to be useful, however it does not meet completely the purpose thus it is used as a comparison rather than for its results alone.

3.4.6 The Slicing Approach

The slicing method was developed with the goal of reducing the need of prior knowledge about the model.

The algorithm's underlined idea is to slice the scan in a longitudinal direction. The thickness of the slices is small enough to provide an almost continuous set of slices. Each slice is modeled as a 2D slice shape. For each slice shape, a polynomial can be fitted. The area of each 2D slice shape is computed.

Considering the thickness of the slice, the volume of the slice is computed. Hence, by means of integral calculus and sum infinitesimal slices' volume, the total volume is computed. The smaller the thickness, the longer the algorithm will take to compute the volume.

This method will allow a fit of the most adequate model to each slice ensuring precision even when handling engraving. Again the more complex the model one fits, the longer it takes for the computation to be solved.

The model to fit has to be carefully selected as it is not desired to obtain an over-fit of the model. Overfitting allows the possibility of taking into account non existing shapes caused by noise.

The slicing method will also allow the possibility of comparing slice by slice the produced mold with the CAD model, making evident where the defects are located with a precision as fine as the thickness of a single slice.
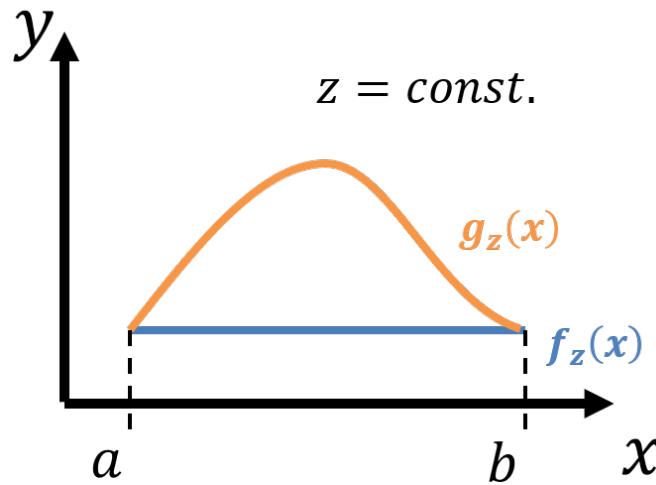
Figure 3.13: Generic schematization of a slice in a mold without concavity

Let $f_z(x)$ be the line corresponding to the cut of the closing plane and $g_z(x)$ the cut of the cavity of the mold.

The area of a single slice located in z in a longitudinal axis is given by the area under $g_z(x)$ minus the area under the curve $f_z(x)$.

$$A(z) = \int_a^b g_z(x)dx - \int_a^b f_z(x)dx \tag{3.52}$$

The volume results of the integration of the areas along the z axis, in a practical case it corresponds to the sum of slices separated by a given distance. The area is assumed to be constant along that

distance, reducing this distance allows the method to be more precise as it reduces assumption of constant section area.

$$V = \int_c^d A(z)dz \tag{3.53}$$

$$V = \sum_{z_{ROI}=c}^{d} A(z) \tag{3.54}$$

with $z_{ROI} \in [c, d]$

As in practice the limit of the cavity does not intersect the closing plane the volume computed will be of the shape closed by two vertical lines as shown in the schematization in Figure 3.14.
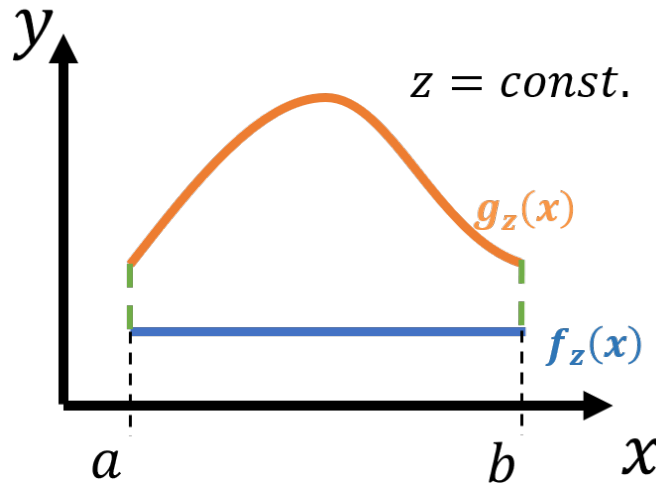
Figure 3.14: Schematization of a slice in a mold with concavity

To measure how well the polynomial fits the scanned curve the Root Mean Square Error (RMSE) is used.

RMSE is commonly used in regression analysis to verify experimental results. It consists in the standard deviation of the residuals, which measure how far the data points are from the regression computed.

$$RMSE = [\frac{\sum_{i=1}^{N}(z_{scanner} - z_{regression})^2}{N}]^{\frac{1}{2}} \tag{3.55}$$

This error allows the evaluation of the result and it also creates the possibility of varying the degree of the polynomial which will allow to avoid over fitting without losing flexibility of shapes when needed, for example when a simple mold has engraved letters or forms in it.

The idea of implementing an iterative solution to find the best fit intends to address computational efficiency and lower time of processing.

In the glass mold industry the most common shape will have the best fit at the second degree polynomial, so the iteration is not expected to take longer than assuming an order for the polynomial.

There's no guarantee that the computational time is going to be reduced since it also depends on the complexity of the shapes nevertheless it is justified by the increase in accuracy needed for this cases.

For this reason a stopping criterion should exist based on a very low value of the RMSE, defined experimentally.

Chapter 4

Implementation

4.1 Technological Solutions for 3D Scanning

A 3D scanner is a device capable of capturing digital three-dimensional information about the shape of an object. It can capture shapes from a small dent on a gear to a real size aircraft. Some can also acquire appearance data such as color.

Commercial cameras and scanners in general were developed to measure distances in a larger scale than the one needed for this purpose.

These devices have applications such as detection of a hand, measuring buildings and even reverse engineering mainly for surfaces reconstruction to create models. Reverse engineering itself has several branches, from the models to reproduce in 3D printers to metrology applications.

Early approaches were able to complete the task using cameras, lighting and a projector, but all of them were limited to the computational effort allowed by computers of the time, making it impracticable to obtain a complex model.

In a quality inspection unit this device allows automation and accuracy that move beyond specialists. In this specific case there is a lot of potential since the current manual procedure is very time consuming and subject to errors as explained earlier in this section.

Several technological solutions were considered to determine the best solution regardless of its cost, therefore it is important to understand the principles behind of each method to predict which ones will have an appropriate performance.

To meet the company requirements in this quality inspection station a solution using a 3D scanning method that doesn't touch the part and that is non-destructive needs to be implemented, according to the classification in the diagram 4.1.

With these specifications the choice is between the non-optical solutions such as acoustic and magnetic and the optical solutions whether active or passive. Several tests were performed with the collaboration of other laboratories.

4.1.1 *Laser* Scanner

A laser scanning system uses *laser* as light source to measure the distance between the sensor and object in scope [15] [16]. By the classification in Scheme 4.1 Laser scanners are non-contact, non-destructive, optical, active systems.
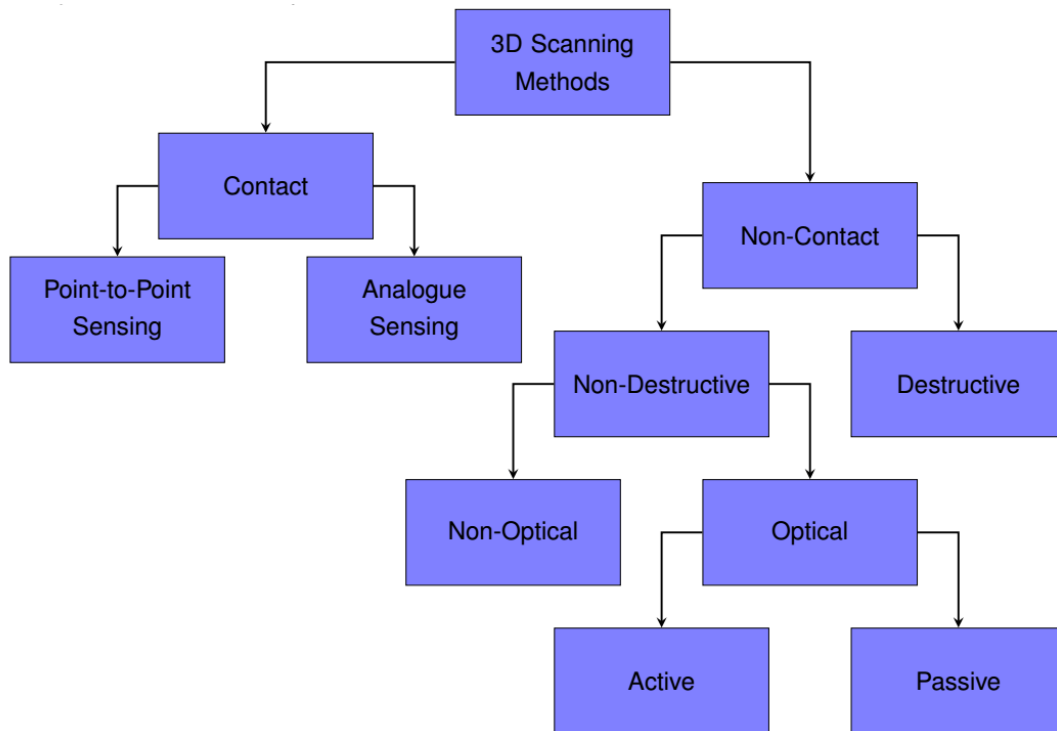
Figure 4.1: 3D scanning methods classification [4], [5]

ZScanner 700 3D Scanner

Lab2Prod at IST and their researchers allowed the opportunity to learn and use their ZScanner 700 for tests, shown in Figure 4.2.
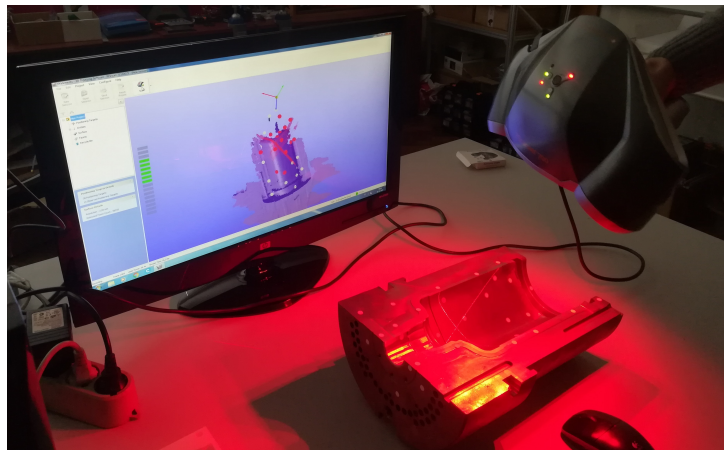
Figure 4.2: Cast iron mold being scanned with ZScanner 700 with position targets at Lab2ProD

The results were promising when tested with cast iron molds although difficult in polished surfaces. Worse results were obtained for bronze molds. As it is noticeable in Figure 4.3, the projected cross is much clearer on a) than on b) where several and successive reflections are observed.

With this device position targets were used in order to overcome the difficulties created by symmetry and talcum powder on the bright surfaces. As the price range of laser scanners is above visible light scanners and its performance experimentally lead to worse results laser scanners were no further explored.

(a) Cast iron mold

(b) Bronze mold
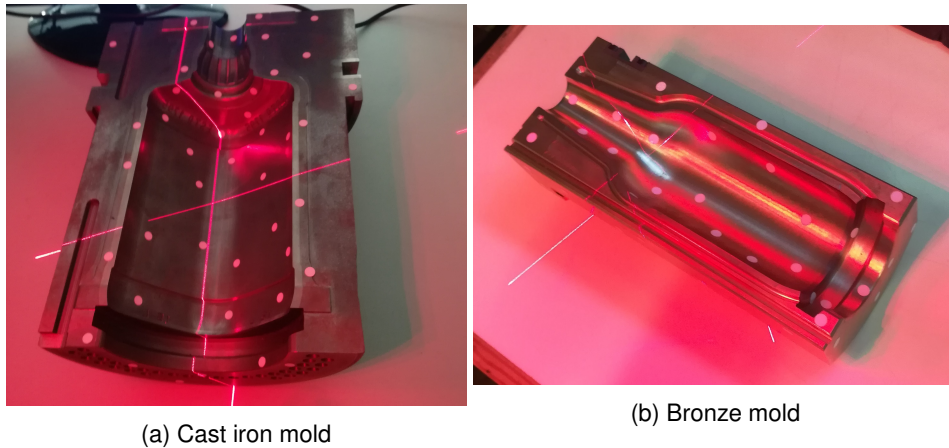
Figure 4.3: Laser projection on different materials

4.1.2 Structured Light Scanner

Structured light scanner systems, in particular the ones which use visible light, are expected to perform well in variable conditions as it is possible to vary the wavelength of the light source. This is a key point when selecting a scanner's light source, as visible light is a continuum spectrum it can be adjusted in a range from 400nm to 700nm to the most convenient wavelengths in order to improve its performance at eachset of lighting conditions [17]. By the classification in scheme 4.1 structured light scanners are non-contact, non-destructive, optical, active systems.

As Dan Perreault [17] states, the higher the wavelength the lower the resolution, meaning the decreasing order of resolution is blue (405-500nm), green (532nm) and red (630-680nm).

Blue light is the preferred for state of the art scanning technologies as it has the highest resolution, it is ideal for dark and reflective surfaces as it needs, in theory, less or no treatment of the surface with sprays or powders. It comes with two main disadvantages as it is harmful for human vision and it is the most expensive of all three options.

One Structured Light Scanner is the Einscan-Pro, *Laboratório de Biomecânica de Lisboa* at IST and their researchers kindly allowed some tests to be performed with it.

An older model, the Einscan-SE was made available for tests by Fablab Lisboa, while attempting tests with one mold difficulties were experienced dealing with the reflections even using talcum powder. A simple experiment was carried out by scanning another object, with different kinds of surfaces. In Figure 4.4 it is observable that both black and metal surfaces were not captured by the scanner, and in both cases no points are placed in the correspondent areas, thus creating a missing data problem. In the case of the black surface, the toy duck's eyes, light is not reflected, so no points are acquired as it is visible in Figure 4.4c.

Solving a missing data problem is not a simple question, since it depends on each particular case, if one knows the error will be recurrent and how to estimate the bias caused by it the problem would appear to have a solution despite the error it would cause. Since the problem in the scope requires a general solution this question will be left open for further investigation that would complement the approaches here discussed.

(a) Toy scanned in the experiment   (b) Point Cloud Acquired   (c) Detail of the result
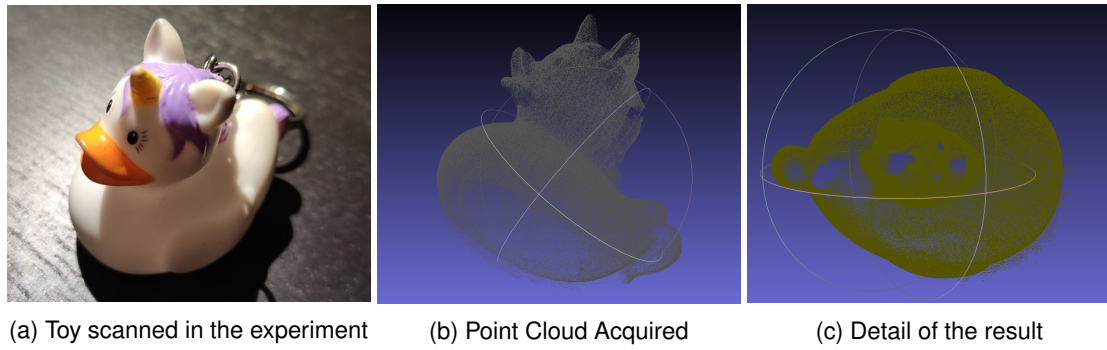
Figure 4.4: Einscan-SE experiment results

Einscan-Pro Handheld Scanner

The Einscan-Pro is a structured light vision system produced by Shinning 3D. It allows four scanning modes that were explored. All the scanning methods required the use of talcum powder to reduce the reflectivity surfaces.
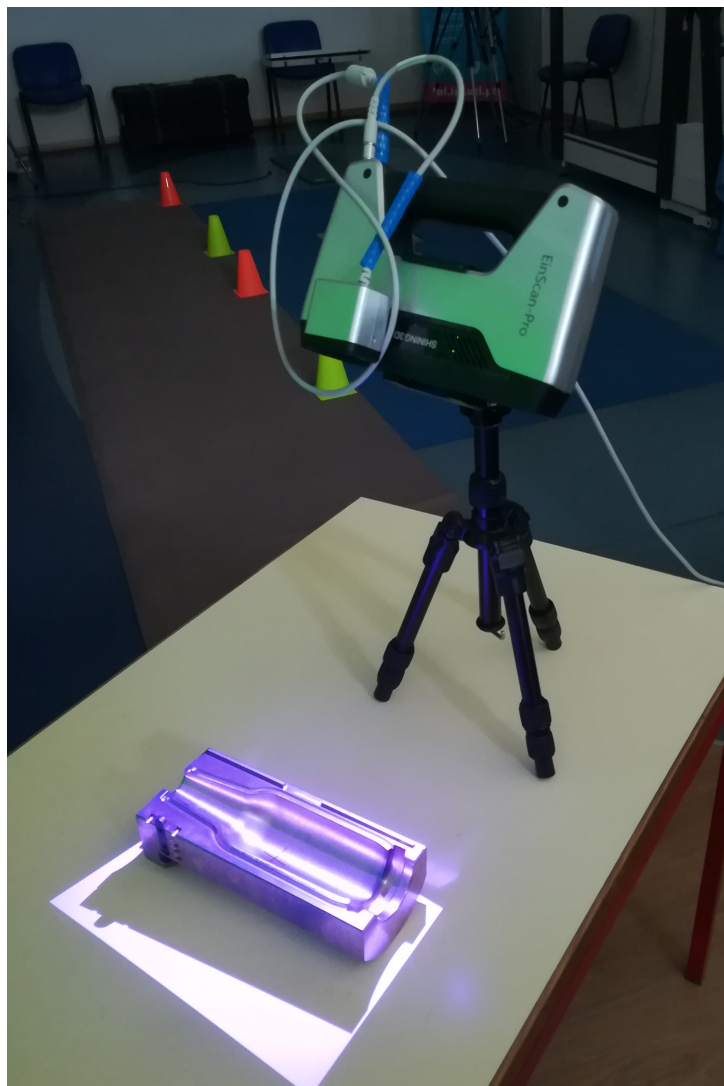
Figure 4.5: Einscan-Pro

Handheld Rapid Scan

The handheld rapid scan is the simpler way to scan and the least demanding in what concerns preparation of an object, of course it has drawbacks as it is the option with less precision.

Figure 4.6: Einscan-Pro in fixed mode

Handheld HD Scan

In this option one has to hold the scanner just like in the Handheld Rapid Scan mode but in this case the object is marked with target points that will allow a faster and more reliable fitting of each point cloud acquisition. The accuracy defined in "Einscan-Pro Quick Start Guide" [18] for this option is 0.1mm. This method was not tested as by experience from the work with the laser scanner it was already known this wouldn't represent a viable solution to the industrial partner.

Automatic Scan

In this mode the object to scan is placed in a turntable that rotates a given angle at an interval of time and stops to make an acquisition. The accuracy defined in "Einscan-Pro Quick Start Guide" [18] for this option is 0.05mm.

This solution was not tested for molds since it has limitations in terms of weight that wouldn't allow to safely scan even one of the cavities.

Nevertheless the turntable option was tested with a bottom part and allowed the conclusion that many occlusions would result and thus eliminated this mode as an option.

Fixed Scan

This Method is the one that guarantees the best resolution, it is illustrated in figure 4.5.

The accuracy for this device in this mode is defined in its Start Guide [18] in the technical specifications as 0.05mm.
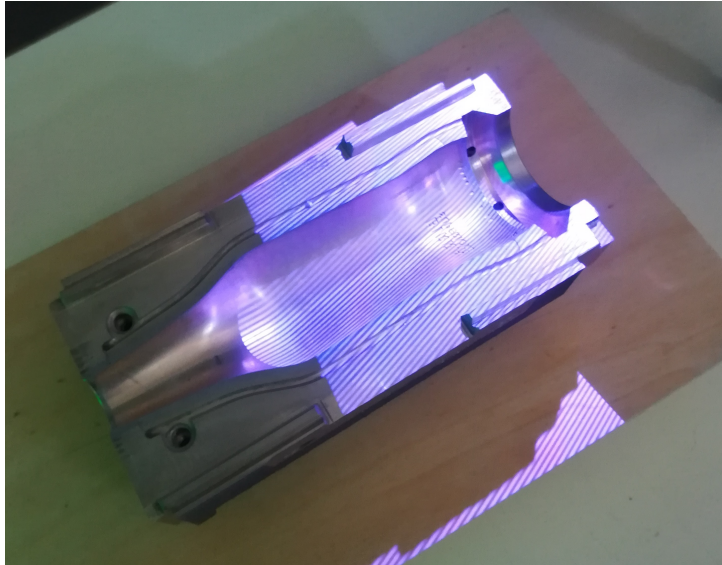
Figure 4.7: Einscan-Pro projected patter in a bronze mold

The procedure consists in placing the scanner in a fixed position for each acquisition, the position of the object has well as the projector can be different at each time. Succinctly at each acquisition it projects a pattern as in Figure 4.7 and measures each point by the distortion of the lines in the pattern. The several point clouds are automatically aligned when their features allow it, the user can doubt that the fitting is correct and manually indicate 3 correspondent points in each cloud to better align it.

Practical Challenges

The usage of these devices allowed the understanding of the method, ICP, that fits the point clouds from each acquisition to form a global model of the part. When the object to scan has symmetries and a low number of features the fitting algorithm fails or proceeds but with errors and has to be manually adjusted, causing more uncertainty.

In order to solve this problem a solution was tested by adding features to the background and then subtracting them with recourse the device scanner software for post-processing. Also background automatic subtraction was tested, this procedure would slow down the algorithm reveling no gain since this scanner couldn't avoid post-processing even with background features.

The background features were tested in the HD Mode and Fast Mode. It was shown that they improve the fitting of the several point clouds, although in the fast mode, the results are less trustworthy since it does not have possibility to manually fit point clouds, introducing the risk of unnoticed errors.

For simplicity of implementation the first solution to add features to the scene was a piece of black fabric. The use of fabrics is not recommended when concerning a real implementation since the features have to be exactly the same during all the scanning process. For real implementations adding a background to the scene will avoid sticking targets to the object.

The rotating table available with the device could not be used as the weight limitation was of 5kg, thus lower than the molds used. Some tests were performed with a lighter part out of scope to obtain a sustained expectation in what concerns the possibility of manufacturing one rotating table for the specific purpose of supporting heavier molds.

4.1.3 Time of Flight (ToF)

Physical Principles

The physical principle behind ToF, as explained in [4], relies on the fact that the electromagnetic radiation travels at the speed of light. It follows that the distance d covered in time interval τ by this radiation is

$$d = c\tau \tag{4.1}$$

The ToF transmitter emits radiation $S_e(t)$ at time $t = 0$ that travels a distance d towards the scene and it's reflected back to reach the ToF receiver at time $t = \tau$ as signal $S_r(t)$.

Meaning the radiation traveled a distance $2d$ in a time interval of τ:

$$d = \frac{c\tau}{2} \tag{4.2}$$

The intrinsic difference between ToF and Structured Light Systems is that the first is occlusion free as it assumes, ideally, that the receiver and transmitter are co-positioned. Opposed to the second which implies two cameras or a camera and a projector allowing occlusions as it is explained in triangulation theoretical principals explained in [5].

The challenging part of working with ToF technology is the fact it relies in calculations involving the speed of light. Remember light travels at approximately 3×10^8 meters per second which means if the object is 0.5 m away from the sensor it will take the light 6.67 nanoseconds to travel the 1 m path to the scene and back.

4.1.4 Stereo Vision

Intel Realsense D400 series

In order to scan the molds a stereo pair of Red, Green, Blue and Depth (RGBD) cameras was used, these are a specific type of depth sensing devices that work in association with a RGB camera, that are able to augment the conventional image with depth in a per-pixel basis.

This model uses a stereo infrared technology, meaning the device has two infrared cameras resulting in better depth accuracy compared to older models. The resolution is also the same for both models: 1280 x 720 at 90 frames per second.

The Intel REALSENSE D415 has a field of view of 69.4 x 42.5 x 77 degrees and a minimum scanning distance of 30cm.

These cameras work by measuring the phase-delay of reflected Infrared (IR) light as an additional method to measure distances.

Both the projector and the cameras of the Intel REALSENSE D430 are covered by a wide angle lens, resulting is a wider field of view (91.2 x 65.5 x 100.6 degrees) and a minimal scanning distance of 20 cm. This model offers Global Shutter technology for recordings without distortion. Global Shutter as opposed to Rolling Shutter is the type of sensor that scans the entire area of the image simultaneously.

This sensor is better suited for tracking moving objects, making it an alternative for Kinect, as Intel RealSense Depth Camera D415 was found out to be the best suited for static applications.

The Intel RealSense Depth Camera D415 is suited for depth and tracking technologies designed to give machines and devices depth perceptions capabilities that will enable them to "see" and understand the world.

This camera includes the Intel RealSense Vision Processor D4 featuring high depth resolution - up to 1280x720 at 30 frames per second (fps), long-range capabilities, rolling shutter technology and a narrow

Figure 4.8: Intel REALSENSE D415

field of view ideal for precise measurements. It is designed for easy setup with USB 3.0 and is in a sleek form factor for portability.

With the rolling image shutter and narrow field of view, the Intel RealSense Depth Camera D415 offers high-depth resolution when the object size is small and more precise measurements are required. Intel RealSense D4 Vision Processor is a high-performance Application Specific Integrated Circuit designed to handle the workload from D400 Series Stereo Cameras.

Figure 4.9: Active Stereo Pair [source: https://daqri.com/blog/depth-cameras-for-mobile-ar/]
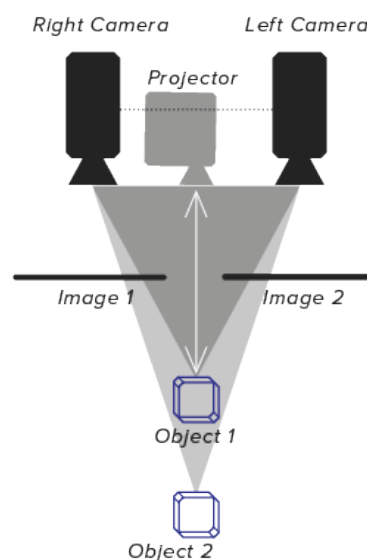
The main characteristics of an active stereo pair, as represented in Figure 4.9 are the minimum distance at which an object as to be from the set, the working area, image resolution and depth accuracy.

When paired with a RealSense Depth Module, the D4 VPU can output depth and full HD RGB data without requiring a dedicated GPU or host processor.

This device is an active pair, which means that it's made of a pair of two cameras with a projector between them, this is called Active Infra-red Stereo.

This setup projects a map of Infrared points that will reflect in a certain object and then the setup computes the difference between the expected and the real position of the infrared points in order to compute the depth field.

The model contains a considerable amount of noise in the acquired depth images since the map of infrared points is not as dense as desired.

4.1.5 Structured Light Cameras

Kinect

Another tested camera was Kinect V2. This model has several applications such as the one proposed in [19] that aims to detect human body parts and in [20] that intends to reconstruct indoor scenes. Preliminary testes made obvious that there was no application in what concerns molds with as much details as the ones described in this section.

For a first approach one can consider a simpler shape with few features either to test the algorithm's or devices' precision. For this reason the first choice of objects to measure were packing boxes. These are easy to find in several dimension ranges and one can easily measure them with a simple and fast method such as with a measuring tape. This next section describes the experiments performed on this objects.

4.2   Box Volume Calculator

The point cloud of the floor taken for calibration is exemplified in Figure 4.10a as the equation of the floor plane is computed. Then the point cloud of the box to measure a top view point cloud is acquired as exemplified in Figure 4.10b.

(a) Point Cloud of the floor for calibration

(b) Point Cloud of the box - top view
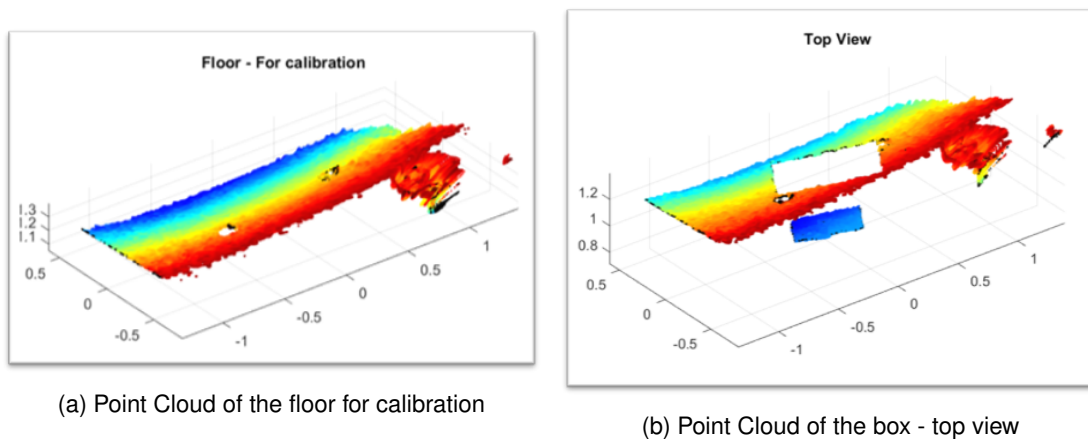
Figure 4.10: Point clouds acquired to compute the volume of the box

Initially the point clouds were obtained from two points of view as in Figure 4.11 and combined with ICP. Two cameras from different points acquire point clouds of a box used as an example of a simple volume.
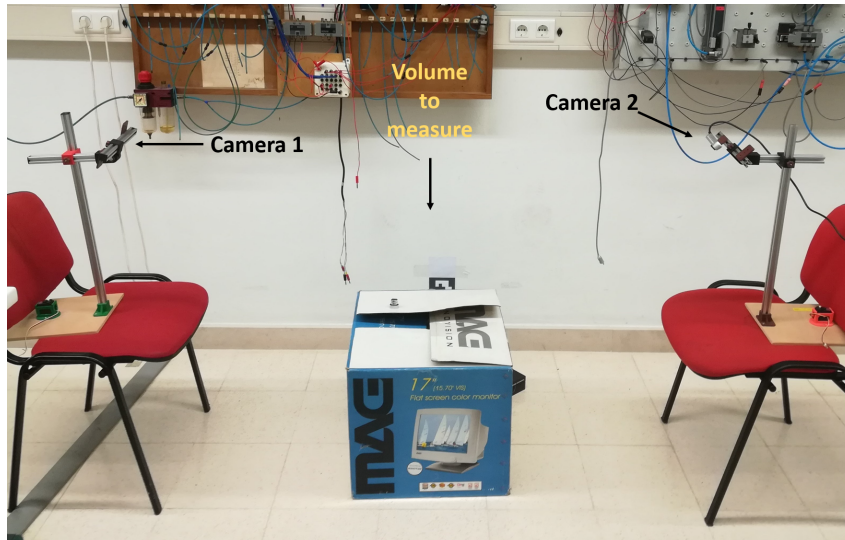
Figure 4.11: Experimental setup for two cameras

Later it was decided to simplify the process using only a top view as in Figure 4.12, using the process described before just for one plane, and determining the height by the length of the normal distance between the floor plane and the top plane of the box.
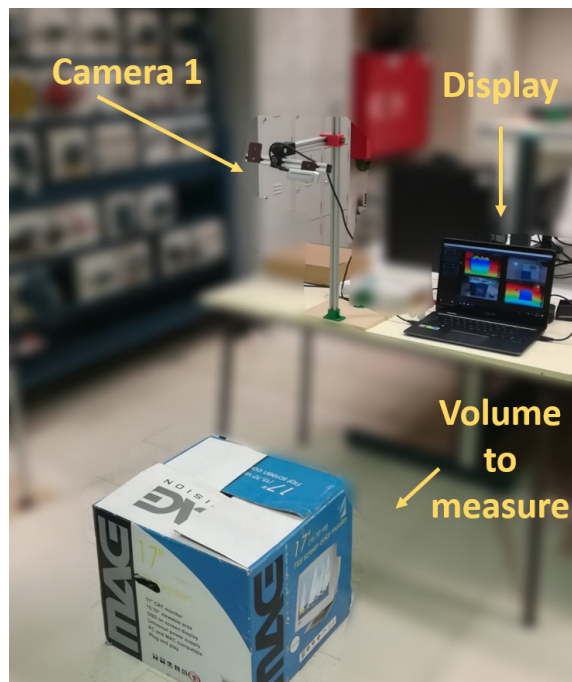
Figure 4.12: Experiment with one camera

4.3   The Feature Recognition Approach

The first implemented working prototype intended to simulate a quality inspection station in a production line and compute the mold volume. Two solutions were tested: one fully automated and one with the assistance of an operator.

Both solutions used data sets from one RGBD camera. Some simplifications were made in what

concerns the shape of the molds and its material.

A prototype of a mold was designed and 3D printed, the shapes were selected to fill in the requirement of having a well defined parameterization.

4.3.1 Goals

To guide the development of this approach some targets were defined and are described hereinafter.

The system is to be capable of measuring the volume of a mold with around $1dm^3$ with 10% precision, using parametric models and RGBD cameras.

It is desired to formulate, implement and compare results for the problem in 2D at first and generalize for the 3D geometries problem.

For testing purposes a 3D model of a simple bottle shape mold is be designed and 3D printed using a mix of known geometries.

Finally it is desired to compare the results obtained in this approach with the ones obtained with implemented reverse engineering solutions as Solidworks, and conclude about concerns for future solutions.

4.3.2 Subsystems

To implement this approach a set of subsystems is required, them being a computer with Matlab 2019, a 3D printer, one Intel realsense D415 and one D435, two support structures and two 3.0 USB cable.

4.3.3 Functional Specifications

The overall system consists of one RGBD camera that scans the mold placed in a predefined position, the data set, consisting of a point cloud, is loaded to the software in order to perform the identification of the geometry of the mold cavity. The parametric identification is done by means of the least squares method for known three-dimensional shapes.

With the knowledge of the shapes and its parameters the volume is computed, presented in the screen and saved to a structure such as a database, this could be done by means of a tool such as Thingspeak.

The mold should be static for the acquisition, so in the case of the solution that uses the conveyor it should detect that the mold is in the center of the image and stop. When the mold is the desired position the acquisition starts, taking approximately 5 seconds (This is done by the implemented pipeline and this time was determined experimentally by observation of point clouds).

The point cloud is pre-processed in order to select the Region Of Interest (ROI) and removing the undesired background. The volume is computed, presented and saved as explained above.

The goal in terms of results for this prototype was an error of under 10% in the measurement of the volume of the 3D printed mold and a computational time of under 3 minutes.

4.4 Obtaining simulated point clouds for Simple Geometries

The idea using simulating data sets is to select parameters of the parametric equations that describe the geometry of the mold, also to simulate the real imperfections random noise is added with a given variance. This means that the points in data set will not be in their exactly expected positions.

Cylinder Data Set

A cylinder is defined by the equation:

$$x^2 + z^2 = r^2 \tag{4.3}$$

Solve for z to determine the z coordinate for a (x,y) grid.

$$z = \pm\sqrt{r^2 - x^2} \tag{4.4}$$

for each (x,y) pair there are two solutions, considering the desired application take into account the negative solution:

$$z = -\sqrt{r^2 - x^2} \tag{4.5}$$
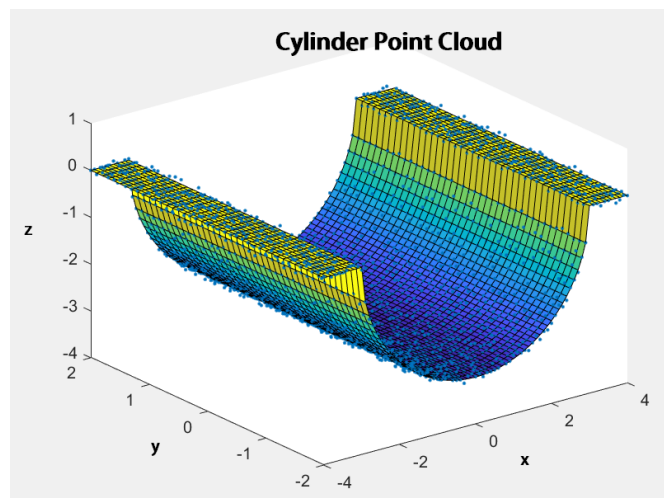
Figure 4.13: Cylinder created point cloud surface with random noise over the exact equation

Ellipsoid Data Set

An ellipsoid is described by the equation:

$$\frac{x^2}{a^2} + \frac{y^2}{b^2} + \frac{z^2}{c^2} = 1 \tag{4.6}$$

Again solve for z to determine the z coordinate for a (x,y) grid.

$$z = \pm\sqrt{c^2(1 - \frac{x^2}{a^2} - \frac{y^2}{b^2})} \tag{4.7}$$

considering the negative solution:

$$z = -\sqrt{c^2(1 - \frac{x^2}{a^2} - \frac{y^2}{b^2})} \tag{4.8}$$
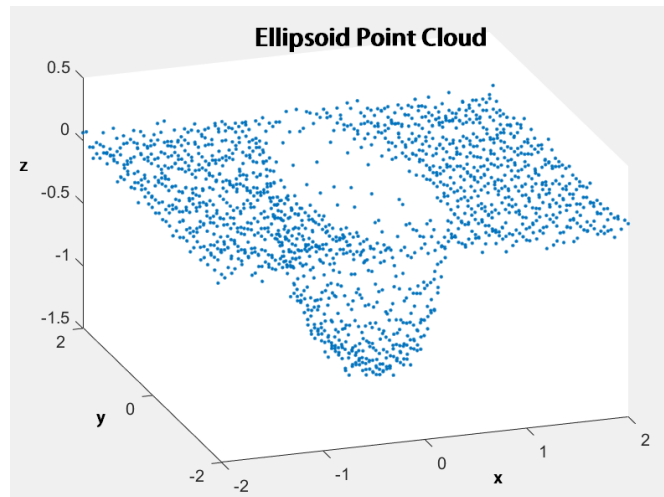
Figure 4.14: Ellipsoid created point cloud with random noise

Sphere Data Set

A sphere is described by the equation:

$$x^2 + y^2 + z^2 = r^2 \tag{4.9}$$

Solve for z and consider only the negative solution as before:

$$z = -\sqrt{r^2 - x^2 - y^2} \tag{4.10}$$
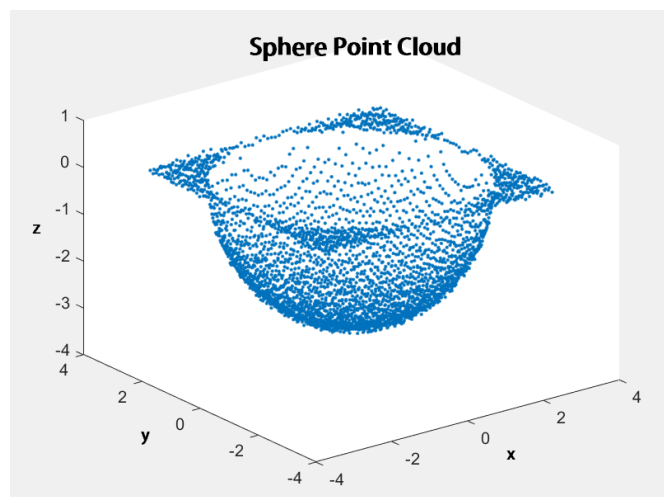
Figure 4.15: Sphere created point cloud with random noise

Cone Simulated Data

Following the same process defined for the other shapes for the cone equation:

$$x^2 + z^2 = r^2 \tag{4.11}$$

Obtain the z coordinates for the (x,y) grid:

$$z = -\sqrt{r^2 - x^2} \qquad (4.12)$$
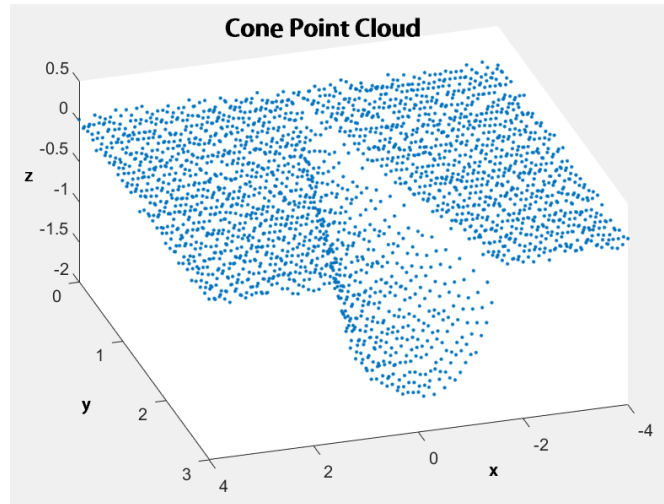
Figure 4.16: Cone created point cloud with random noise

4.4.1 Simulated Random Noise

It is relevant to study how noise affects the model and where the noise comes from in order to be prepared for it and, if possible, reduce it.

Since noise is expected to appear in the range of the camera resolution, it has to be added to the simulated point clouds.

After having the z coordinate with respect to x, y and the respective parameters, which corresponds to the exact location of the points, the random noise is introduced.

In the implementation in matlab random number is summed using rand function which returns a single uniformly distributed random number in the interval (0,1). In order to get a maximum deviation of 0.1 it is divided by 10.

In order to create the signal + , - or zero deviation the random noise is multiplied by randi[-1,1]. This has 3 possible outputs -1, 0 or 1. This procedure is repeated for every shape.

4.4.2 Point Cloud of the Scale Bottle Mold

An important point in this project is to define a bottle to use in simulation which will have the same shape of the one to print in the 3D printer.

In order to have a mold with a bottle shape combinations of simple geometries presented in the previews section, dimensions found to be reasonable for a real bottle were considered. These dimensions may have to be reduced because of the limitations of the available 3D printer.

This mold was created parametrically and for that reason can be reproduced in CAD software, also it is important to have a reference for exact volume. This allows to check if the defined specifications are being met. It is now important to detail the method for parameter checking.

In order to match the limitations of the 3D printers available the dimensions of the model have been adjusted reaching to a final CAD model and correspondent simulated point clouds.
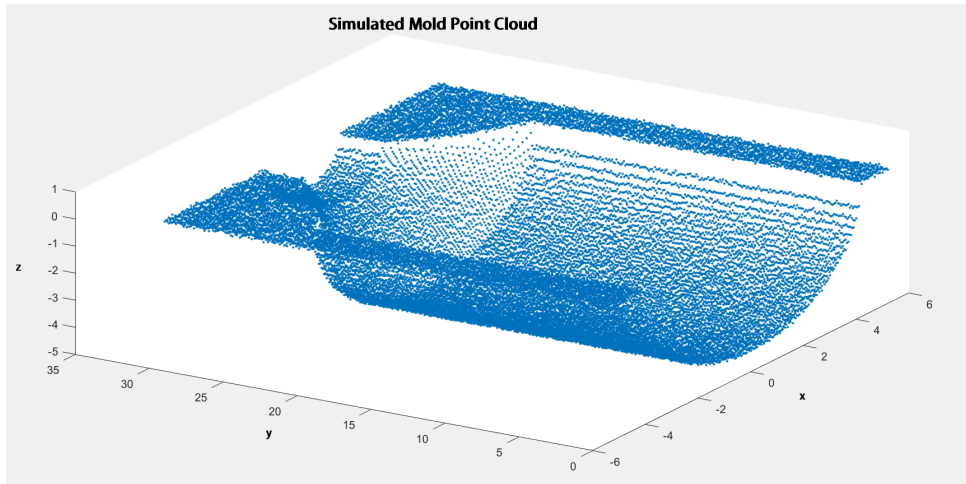
Figure 4.17: Point cloud of the scale bottle mold

A set of point cloud files was created with different influences of noise that can be loaded to matlab and to the calculator.
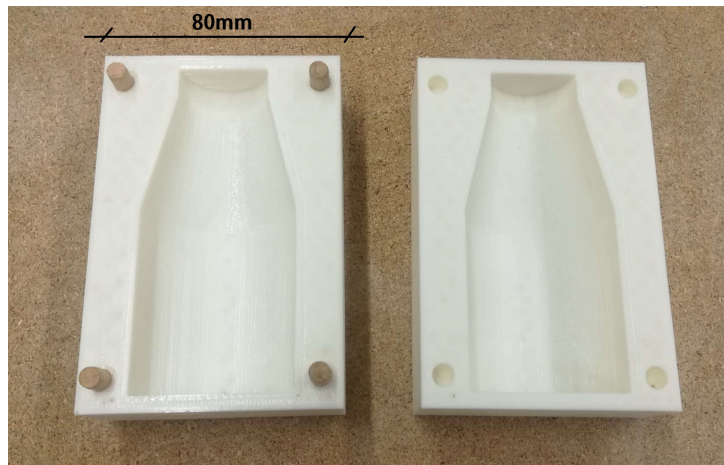
Figure 4.18: 3D printed parametric mold

4.4.3 Analytic Volume Calculation

This volume is used as reference, and it'll be determined by using an analytic method of considering the revolution of geometric figures as all the molds to be considered in this phase are symmetrical.

4.4.4 Practical Considerations

In the implementation of the solution several issues must be taken into consideration. Firstly most of the illumination surrounding the system translates into unwanted reflections of the Infra-red map which will result in incorrect measurements.

In a first approach, images were acquired in a closed dome specifically designed for visual quality control, more specifically in the production line setup in the ACCAII laboratory in Figure 4.19.

Although it reduces the external light influence, it also produces spurious reflections. The later revealing more importance than the former.

Unfortunately, this has shown to be a non-satisfactory solution since, as mentioned before, this solution presented several unwanted reflections which lead to errors in the measurements.

Furthermore, since this laboratory is used by quite large group of colleagues, it was always impossible to leave cameras in the setup, which lead to different positioning of the camera every day and consequently inconstant results.

The conveyor and the structure associated to it are used by students of IST and for a considerable period it was only possible to use the setup for short periods with the need to remove the camera from the setup and re positioning it every time in order to change to the camera the other students where using. It was necessary for the facility to be available to work on the project before or after the periods when this students were present, but no access was granted.
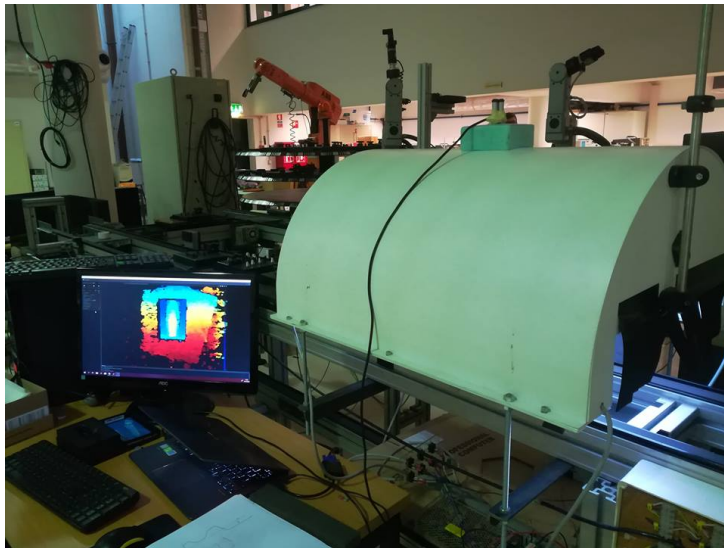
Figure 4.19: Initial setup

Taking all of this into consideration another solution had to be reached, another setup was used, it consisted of a structure with a flat grid surface and an adjustable holder which is able to increase parallelism between the surface and the image plane. The purpose of the grid is to know the absolute position of the mold placed in the flat surface making it possible to compute the absolute coordinate of any point, based on geometric transformation.

The adjustability of the holder is extremely important since the part must be within a range of 30 to 40 centimeters of the camera, otherwise, some points of interest might be discarded.

Two relevant aspects of this new apparatus are the fact that it possesses a level bubble in the basis of the holder allowing the user to know if the setup is leveled or not and that the color of the surface must not be black since the acquisition system has shown some problems with this. For this reason a white grid was placed under the mold as shown in Figure 4.21.

This configuration allows the user to know the precise position of the mold, the height of the camera (with respect to the surface) and, most importantly, allow a stable and repetitive environment of data acquisition.

Noting that in this new solution the orientation of the mold must be constant (top of the mold facing the basis of the holder).
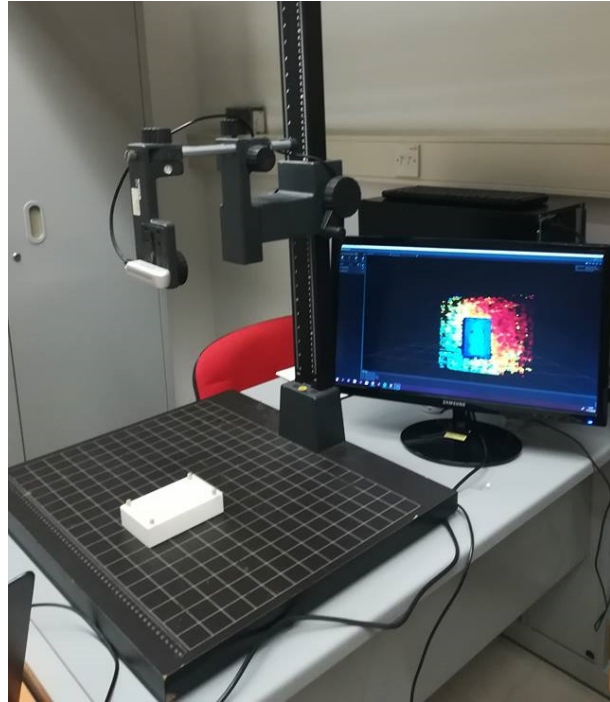
Figure 4.20: Experimental Setup
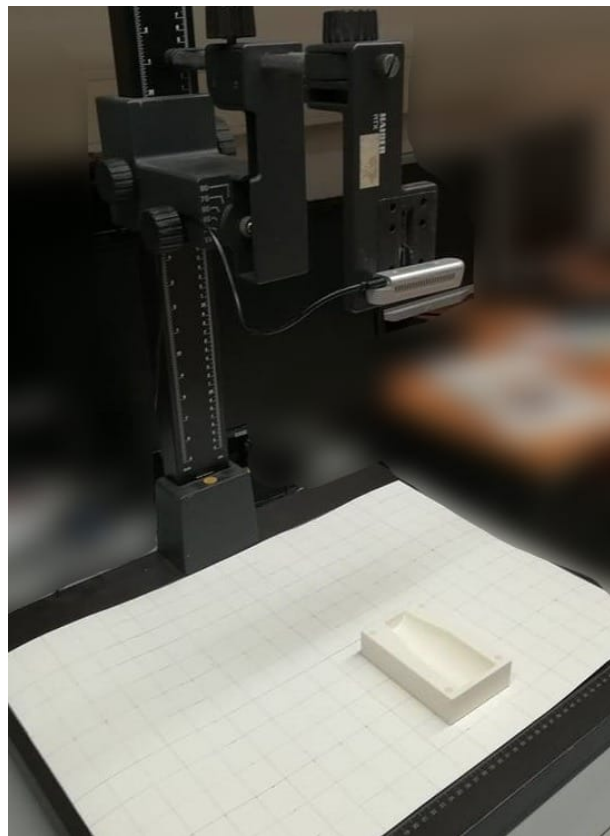
Figure 4.21: Final setup

Software

Two functions were developed, both are based on the one developed for the simulation. Several improvements and modifications had to be done considering the issues found with the real camera data.

The 4 main steps are image acquisition, segmentation, orientation and volume computation.

The difference between the two functions is on the volume computation as one assumes the longitudinal lengths along the height of the bottle, allowing to apply the approach to molds in which the segmentation of the bottom is not straightforward in this level of camera definition, as the other is able to compute these distances itself. The second one was chosen as it computes all the parameters required as it was possible to implement for this kind of molds.

Both return to the user the volume computed in mm^3, the error related to the original CAD model, the error related to a fill tool available and the main radius of the mold.

A simple visual interface, shown in Figure 4.22, was developed in order to simplify the process.
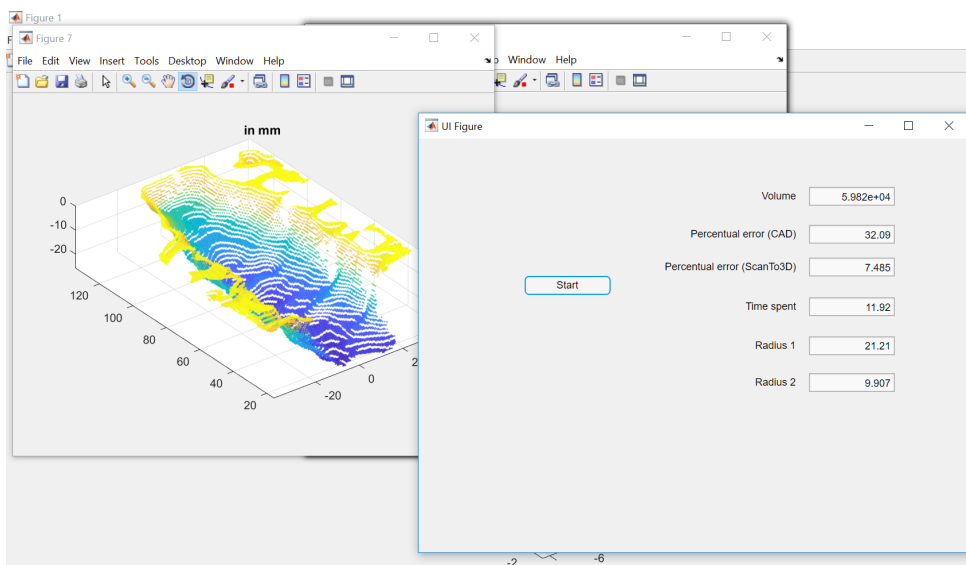
Figure 4.22: Graphical App

None of the functions require any inputs since they are already set to acquire the image for this specific camera, assuming all the procedures described on the setup have been followed.
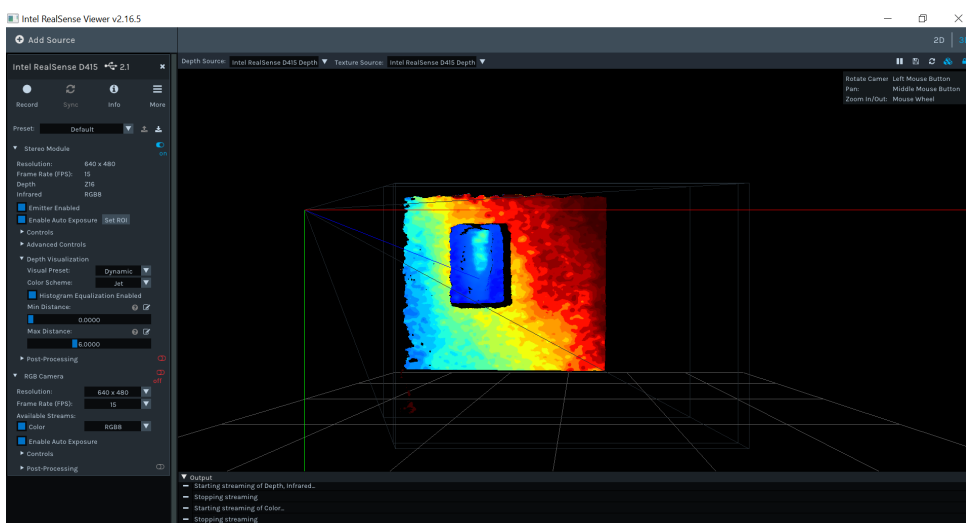
Figure 4.23: x,y Origin Placing

Both the matlab function and the graphical app can be used, either by pressing start on the app or running the function.

The critical step of the ones mentioned above is the placing of the origin belonging to the mold, the remaining steps are not mandatory but will improve the performance of the method.

4.5 The Profile Revolution Approach

The profile revolution approach was implemented by uploading a point cloud of the mold previously scanned. Resorting to ICP a plane is fitted to the top of the mold and the profile is determined. The distance between each two corresponding points in each side is computed and assumed to be the diameter of the circular section.

Obviously this only computes volumes of circular sections. There's also another issue since the diameter is smaller than the one of the rest of the section as it is required by mold designers for technical reasons. This method fails when used with Intel Realsense's scans since their problem is precisely in this top profile corner.

4.6 The Slicing Approach

The slicing method is the most general and further developed approach in the scope of this project. Several variants were developed before reaching a solution.

Two point clouds are uploaded to Maltab, one of the complete scan of the mold that must include the horizontal top of the mold and the same scan but this time only containing the cavity, in the same coordinate system, no new scan is required, only a manual removal of points with no relevance to the interior shape of the cavity. This is being done either with the scanner's software, of which no license was available, or Solidworks that is less effective dealing with point clouds.

The user must select at least three points, three is the desired number to define the plane, that defines the vertical top of mold to which the mold is considered to be filled when using water. These points are not arbitrary and require knowledge of the operator. Generally they correspond to regions close to the corner but this is not a general rule and depends on the design intended to the mold, a reference table is recommended to be developed and available in order to help the operator and reduce the need to rely on his knowledge and memory.

The three points allow the computation of the parameters of the plane by them defined, and points are created in coordinates directly vertical to the ones in the cavity point cloud.

The new points and the existing ones are saved into a new point cloud structure in order to start the actual slicing procedure.

The mold is processed through a longitudinal direction in steps of 0.1mm, this value can be varied, and the 2D parameters of both the line defining the plane and the polynomial defining the cavity are determined, the integral under each line is computed and the difference times the thickness of the slice corresponds to the volume of a slice, in this case it corresponds to the volume of a 0.1mm thickness slice.

The slices volumes are then summed, only considering slices between the two manually selected horizontal planes that close the mold.

User Interaction

The need for a manual region of interest selection emerged by the observations of the range of molds produced by the Industrial Partner and by the glass industry in general.

The plane from where the mold is filled and the plane up to which the volume must be considered is not trivial as it implies the operator knowledge.

The Industrial Partner suggested a manual selection by the operator which was developed, it is obviously subject to human error.

In case the operator suspects an error of the algorithm in the selection of the ROI there is the possibility of using only manual selection.

Selection of the interest points is not obvious but it is necessary as the bottom part of the mold is the hardest to scan and not always possible as it has many occlusions in spots of difficult access to the light.

Chapter 5

Results

In the previous chapter the implementation phase of the approaches was described. In the upcoming paragraphs the results of the implementation are shown and a detailed comparison between methods is discussed.

As a first reference, box measuring results are presented. As mentioned before this experiment and approach in specific was carried out with the main purpose of obtaining a reference for the error in shapes with an accurate manual measurement method to be taken as reference.

5.1   Box Volume Calculator

The box volume calculator concerns a first approach designed to measure the volumes of boxes to test the data acquisition performances. The detailed results for this experiment are presented in Table 5.1. The results would benefit if the camera was placed parallel to the background plane, in this case the floor.

Although the main goal was to return reference error values, some criteria to keep the solution industry oriented were considered, such as the goal to have fast results thus balanced computations between time and accuracy.

Also some assumptions can be discussed further in an industrial implementation of a similar method, in which one can consider standard box sizes and predefined orientations that would allow a time consumption reduction, or an increase of the precision maintaining the time to take the measure constant.

Table 5.1: Results for the box measure experiments

	Real Dimension (cm)	Test 1 (cm)	Test 2 (cm)	Percentage Error
Width	47.00	45.12	44.25	4.93%
Depth	49.50	49.22	49.34	0.45%
Height	41.50	43.31	43.04	4.09%

The Real Dimension is considered the one measured with a measuring tape, with a precision of $\pm 0.5mm$.

5.2 The Feature Recognition Method

5.2.1 Dimension of the Point Clouds

In order to study the influence of increasing the number of points in the point cloud used in the computations experiments were performed with three different point clouds. The results are presented in Table 5.2.

Table 5.2: Number of Points in the Cloud vs Computation Time.

Number of Points in the Cloud	12555	49105	194205
Computed Volume (mm^3)	87535.465017	88076.371181	88545.858941
Percentage Error	0.635150 %	0.021146 %	0.511787 %
Computation Time (s)	1.528571	1.798104	4.419078

The performance in terms of precision of the algorithm is influenced by the random noise in the point cloud and not only by its dimension.

This experiment intends to determine the range of the Time Elapsed during the computation, and as it can be seen the time is increasing when the number of points increases, as expected.

It's important to have in mind that times are measured for the point cloud load and not obtained by the camera. To be noted that a scan obtained with a 3D commercial scanner has around 4 million points.

Also it can be seen that the performance in terms of precision is not compromised since there is a 10% tolerance and the error is around 0.5% in simulation.

5.2.2 Volume Reference

A reference volume for comparison had to be determined by an alternative measuring methods since the volume of the CAD model would not account for the errors in the production.

Since it is relevant to measure the performance of the algorithm, and not the performance of the 3D printer, the approach was to know the actual volume of the printed mold resorting to Solidworks' tools.

The coordinates of the points acquired with Intel Realsense were uploaded to Solidworks and a process of "filling" the mold with another solid volume was performed, by means of subtraction of solids. The surface and solid obtained is shown in Figure 5.1.

In Figure 5.1 it is shown the result of the uploaded point cloud in Figure 5.5, processed by Soldiworks' algorithm to approximate surfaces from point clouds and to close those surfaces.

Due to missing data, clearly illustrated by Figure 5.5, in the upper cavity zone that Solidworks was not able to extrapolate in a reasonable way, it was not possible to account for all the volume, the value is under its real volume giving a result of $61584mm^3$.

This procedure requires point cloud manipulation which is not general for all the point clouds and is time consuming, thus it can't be performed with macros if the scanning has this missing data that can't be extrapolated by the software correctly, also the scanning process has to remain standardized.

The method of measuring the volume with water was also tested, but due to several holes in the plastic structure that was not viable. The measure could have been taken with a modelling clay of known density.

Figure 5.1: Solidworks volume
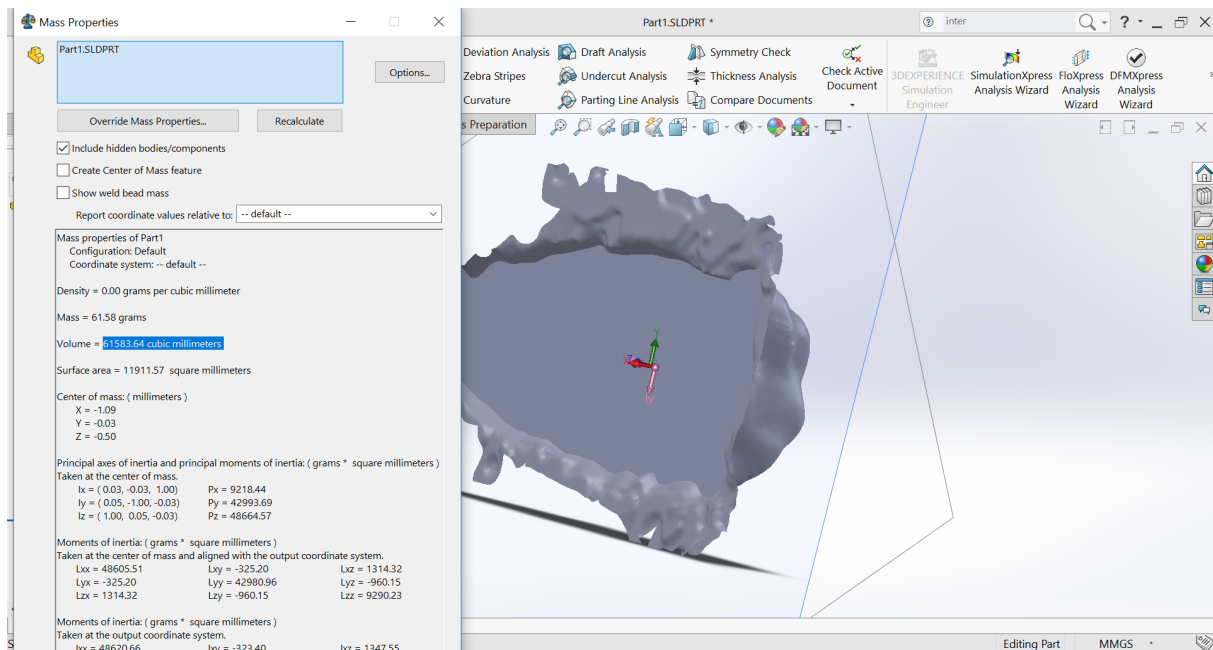
5.2.3 Display to the User

The result of the method can be presented on the command window on which the function is used or directly in the graphical application.

Either way several plots are displayed in order to detect possible errors in image acquisition or processing, this is a key feature since the method is yet being tested.
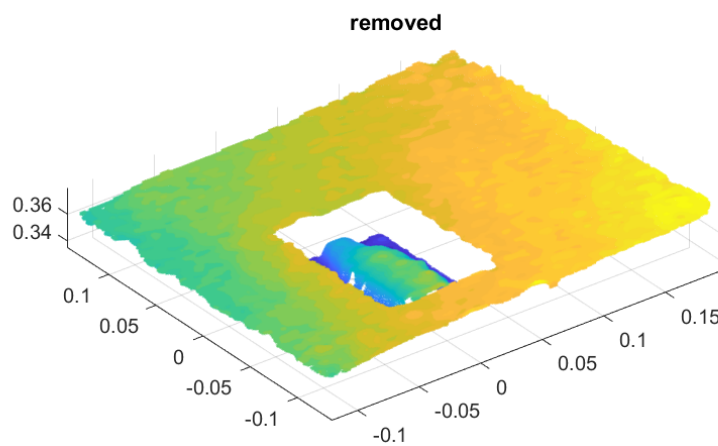
Figure 5.2: Point Cloud Obtained seen from bellow
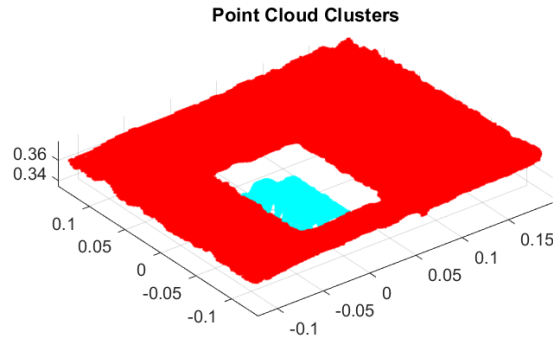
Figure 5.3: Clustering to select the mold, the cluster that contains the x,y origin

The code does not display errors by itself. In case of error, for instance if the mold is not placed in the origin, the method will fail but it is possible that a value is returned if no Matlab error occurs. In this case the algorithm will be trying to fit the background plane in the shape of the mold and the percentage error will be above the expected. This is an alerting sign that a logical error occurred.

The other possibility in this case is if, for instance, the camera is placed outside the desired distance range and every point in the point cloud is deleted along the first steps of the code, in this case a Matlab error will occur because it will not be able to do necessary computations.

Figure 5.4 shows the use of the Iterative Closest Point (ICP) to rotate and position the point cloud in a standard position by means of the transformation matrix computed by this method.

Figure 5.4: Orientation of the point cloud using ICP

The developed prototype represents the first experiment performed in which the shapes are similar to real molds introducing a new level of difficulty, thus to approximating the experiment to a potential industrial solution, nevertheless one relevant factor of interference differs from glass molds: its material.
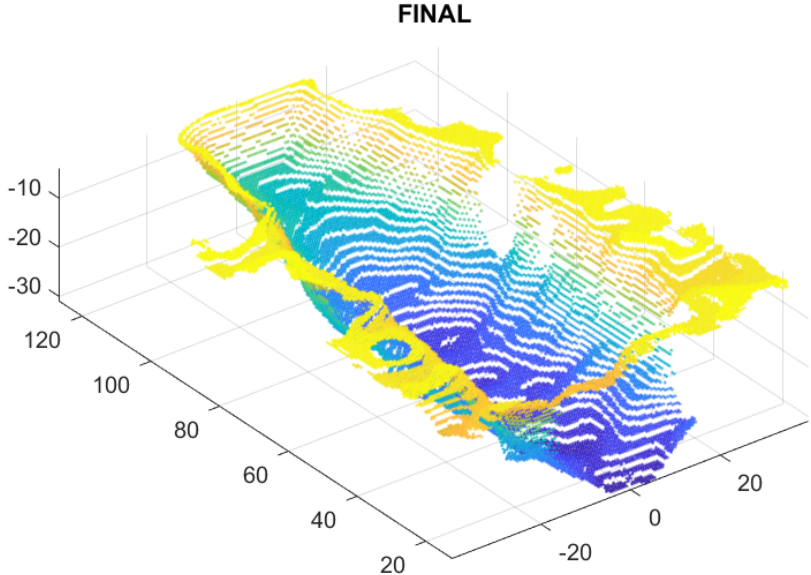
Figure 5.5: Point Cloud that is going to be used in volume computation

5.2.4 Method Overview

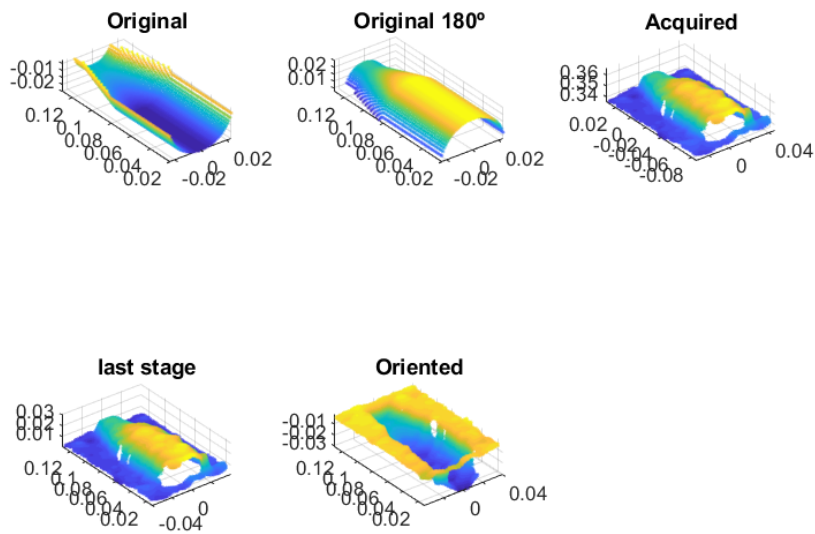The focus was on testing the implementation performance rather than to quantify the quality of the mold printed. Once a final solution is tested and considered functional the implementation will be focusing on the quality control of the mold produced, by returning a mold volume, an error and an uncertainty of the measure calculated during the testing.

The development and implementation of this method were analyzed. The idea showed to be promising for simple geometric shapes which is not the case of typical molds for the glass industry as it is explored in Section 2.

The first approach was the use of Intel, thus in this chapter Intel Realsense D400 series cameras were used for all the acquisitions, although they can have multiple usages, they do not have performed with the precision required to achieve the desired goals for these approach. As stated in section 4.1.4 have its best results in determining location of larger scale objects.

As it is possible to observe in Figure 5.5 the data shows non-existing shapes with appearance of defects, this factor led us to search for better accuracy devices, thus it was decided to explore 3D scanners.

Figure 5.6: Results of the feature recognition method

5.3 The Profile Revolution Approach

The Profile Revolution intends to meet the specifications in terms of time by taking the assumption that mold shapes are the revolution of a profile.

This approach begins by registering the top plane of the mold using ICP. The top plane is rotated and aligned with the x,y plane. The profile lines in each side of the cavity are identified, allowing to compute the distance between them. In the case of a cylindrical shape this distance corresponds to its diameter.

Infinitesimal volumes are computed and summed to obtain a total volume. The operator has to manually select the limits of the cavity region of interest, since no general criteria was reached.

Table 5.3: Results for real point clouds using the Profile Revolution Approach

Ref.	Result (cm^3)	Nominal Volume (cm^3)	Absolute Error (cm^3)	Percentage Error
0561	414.60	417.00	2.40	0.60%
2283	416.76	418.10	1.34	0.32%
11937	163.49	166.19	2.70	1.60%

This method is significantly faster than The Slicing Approach, as this takes less than 2 minutes to compute a volume, reducing the amount of data of input that is not used would make the processing time less than 1 minute and it would also benefit the registration of the top plane.

The main limitation of this method is that it does not take into account the entire cavity of the mold but only its profile, meaning it does not account for engravings or cavity defects. Also it depends on the operator action.

Testing this method allows relevant conclusions, not only about the method in particular but for general development of a solution. In an infinitesimal volume of $0.1mm^3$ and for a diameter of $6cm$ typical for a mold of a 33cl bottle, for Einscan Pro's mode with the smaller uncertainty $0.05mm$, assuming there is no error associated with registration of several point clouds, the error caused by this uncertainty is around $1mm^3$. In a entire mold of a 33cl bottle this would represent an error of $2cm^3$.

In order to obtain an uncertainty of $\pm0.1ml$ for a 33cl (remember that mold filling has an uncertainty of $\pm0.1ml$ for a 100ml mold) the solution would need a scanner with accuracy of 0.015mm which is the accuracy of the RobotScan E0505 from Shinning 3D, a solution that combines a robotic arm and a scanner from Shinning 3D, but is out of the price range of commercial scanners.

The manual selection related uncertainty is also a concern, as different types of molds would require different criteria to select the limits of the region of the mold that should account for the volume, as the Industrial Partner has suggested. Due to manual selection an uncertainty of $\pm 2.5 cm^3$ has to be considered, it is understood that if this solution is to be used in an industrial environment a zoom tool would be crucial to reduce this uncertainty, as the Matlab graphical interface for the selection of the points does not allow the user to zoom, adding difficulty to a subjective task. Nevertheless, an automatic selection with a general criteria would benefit the repeatability of results.

5.4 The Slicing Approach

Results were obtained for different scanning of molds. As, in general, only one scanning of each mold was available and from only one mold of each reference, there wasn't the possibility of checking for a tendency in the results, thus the focus is on absolute results. A comparative test is performed with only 3 molds that were available.

The first approach was again with Intel Realsense D415 for the simulated mold created in the 3D printer in Figure 5.1. As it was observed in Figure 5.5 there was a lot of missing data and for that reason it is difficult to have a reference for volume, as rapid prototyping has a low level of compliance with the CAD model.

For this reason new scanners were tested with industrial molds and the solution was compared between them. Starting with a 1,5l whiskey bottle mold in Figure 5.7 from the Industrial Partner, both Intel Realsense D415 and ZScanner 700 were tested. Also Infaimon performed a test on the same mold with its "Profile Laser Sensor" from LMI GOCATOR 2350, the results are presented in Figure 5.8.
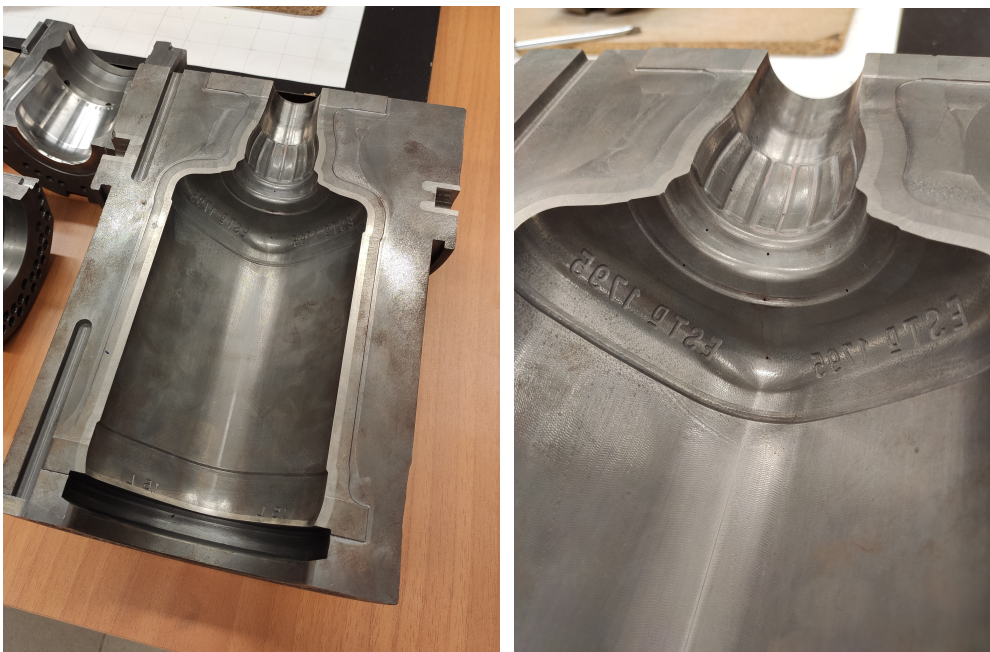
Figure 5.7: Whiskey bottle mold

As it is observable in Figure 5.8c as the cameras are placed perpendicular to the mold there are surfaced that are not registered. Thus the method would fail as it is developed for occlusion free scanning methods. This device would not allow to inspect the full interior surface of the mold.

It is also possible to notice differences between Figures 5.8 (a) and (b), as the second is clearly better. It is relevant to state that Intel Realsense D415 is in a price range around 150 times lower than

(a) IntelRealsense D415

(b) ZScanner 700

(c) Profile Laser Sensor
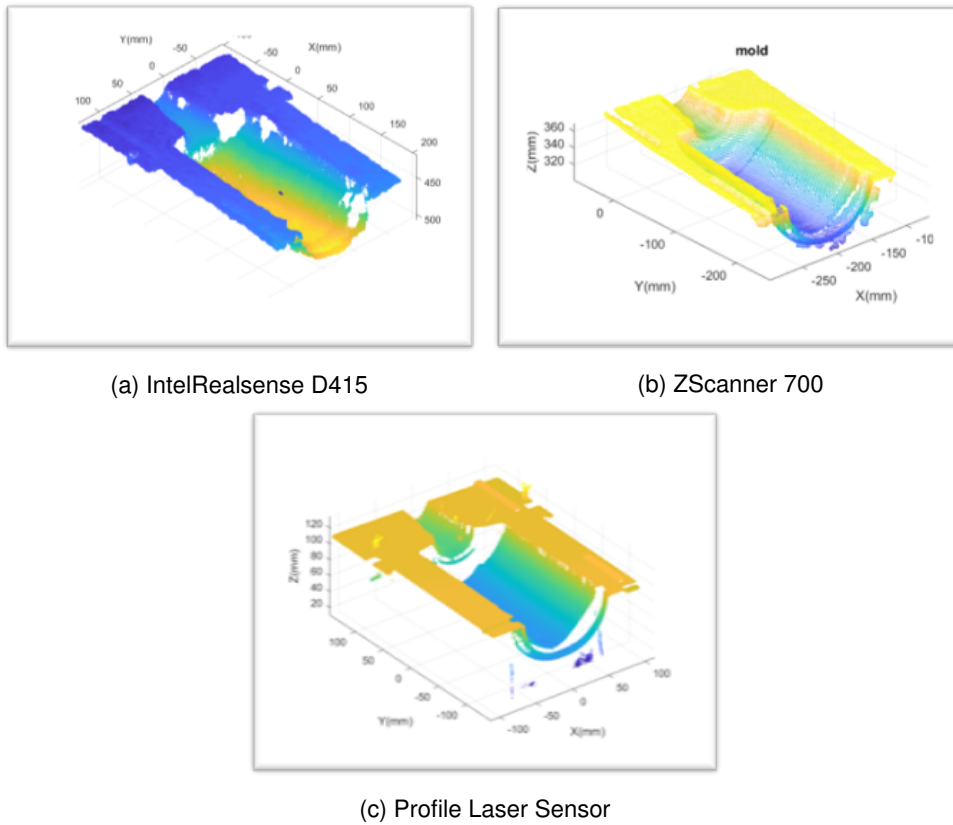
Figure 5.8: Comparison between the point clouds for the same mold and for different Scanners

the ZScanner 700.

The results can also be observed in the accuracy of the slices, as shown in Figure 5.9.

(a) IntelRealsense D415
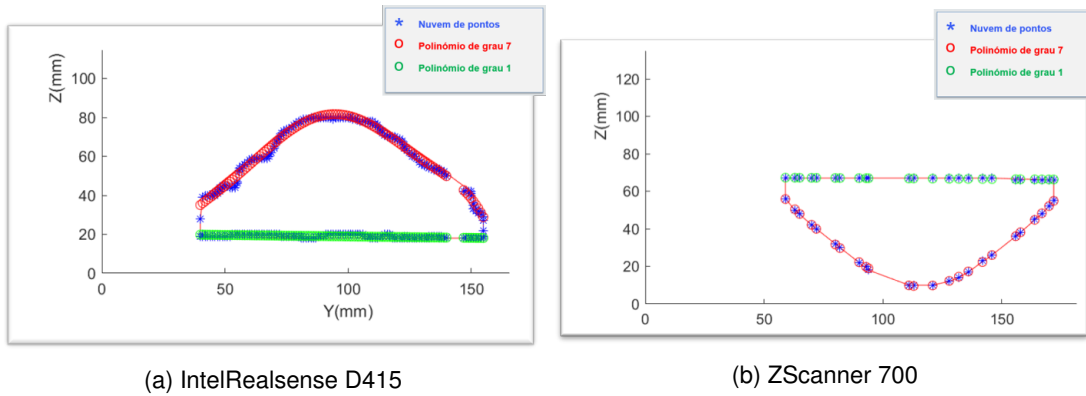
(b) ZScanner 700

Figure 5.9: Comparison between the slices for the same mold acquired with Intel Realsense D415 and ZScanner 700

The internal volume of one cavity was computed for both solutions, the volume used as reference is a mere guess done by the Industrial Partner as they consider the 1500ml of the bottle filling, plus 400g of glass, then one has to account for the space correspondent to the bottom part.

Considering a glass density of $2500kg/m^3$, 400g of glass correspond to $160cm^3$ ($1cm^3$ corresponds to 1 ml). Since this is an approximation it will be considered 25% of the bottle volume to account for the bottom part and also the part of the bottle that is empty, giving a total volume of $1017,5cm^3$.

The results obtained by the slicing method are presented in Table 5.4. Although the percentage errors are just an indication and are not exact it illustrates the idea of how much does a better scanner

influence our results.

Table 5.4: Results for real point clouds of an 1,5L bottle mold.

Scanner	Intel Realsense D415	ZScanner 700
Guess Volume (cm^3)	1017,5	1017,5
Computed Volume (cm^3)	951,2	1019,2
Percentage Error	6,5%	0.2%

The next step was taken using EinScan-Pro to obtain point clouds of two molds from different references, meaning 4 cavities were scanned. The setup in fixed scan mode for this acquisition can be observed in Figure 4.6. In Figure 5.10a it is possible to see that there is missing data in the bottom part socket. This was the main reason that made us spare the quality inspection in this region, as data extrapolations would add data with no physical meaning.

(a) Male

(b) Female
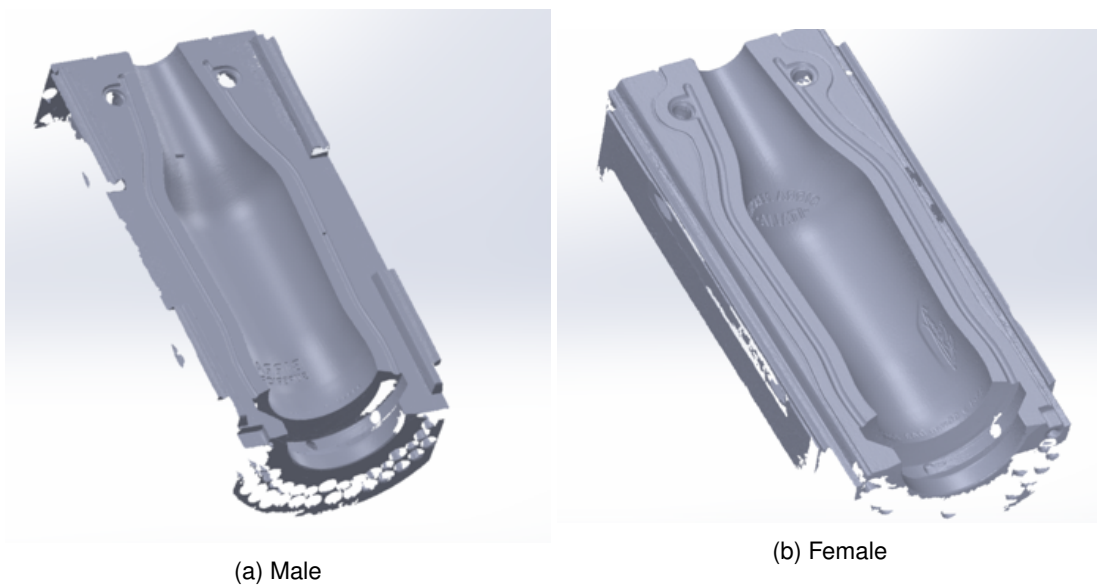
Figure 5.10: Acquisitions in Fixed Scan Mode - Ref.2283 - 33cl bottle

A bottom part was also scanned with this device to test the Automatic Scan, as this is the only part which weight can be supported by the turntable. The Automatic Scan mode has shown not to be a solution when considering molds since it has a large area of missing data as it can be observed in Figure 5.11.

(a) HD Handheld Rapid Scan mode

(b) Automatic Scan mode
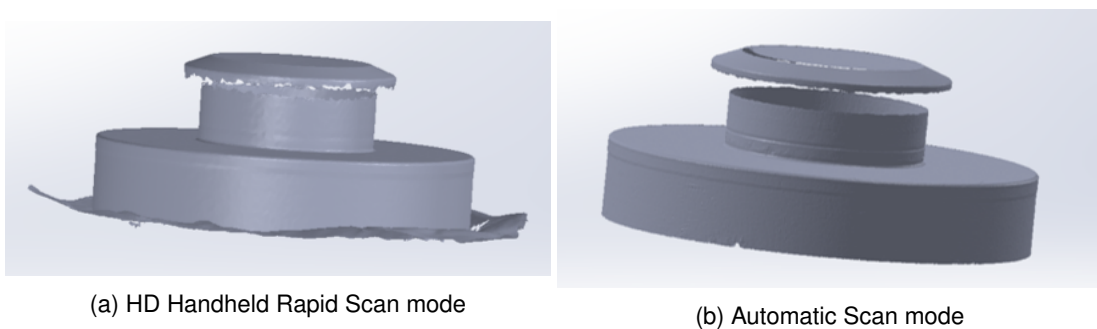
Figure 5.11: Acquisitons of the bottom part

Two point clouds were obtained for one of the cavities of ref. 0561, a symmetric 33cl bottle mold. One acquired with Intel Realsense D415 and the other with Einscan Pro. An exemplification of the slices

in each one is presented in Figure 5.12.

(a) Intel Realsense D415
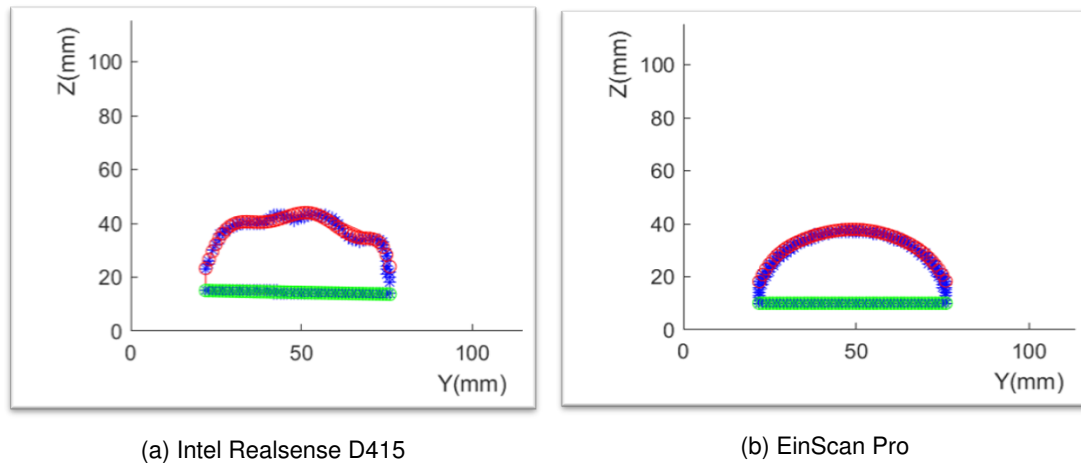
(b) EinScan Pro

Figure 5.12: Comparison between the Slices for the mold with ref. 0561 acquired with Intel Realsense D415 and EinScan Pro

Results presented in Table 5.5 were obtained for the mold with Ref. 2283 for the Einscan Pro point clouds. This Table and Figure 5.12 show also what was already stated about Intel's cameras as it seems to create non-existing surfaces and reducing the volume.

Table 5.5: Results for real point clouds of Ref. 2283.

Ref.	2283
Real Volume (cm^3)	418,11
Computed Volume (cm^3)	209,77 (male) + 212,07 (female) = 421,84
Percentage Error	0,89%

This result was obtained with the method of automatic selection of the plane where the bottom part fits. This is done by finding the maximum of the second derivative.

The selection is presented to the user as in Figure 5.13 where the red line is the second derivative and the blue line is the mold profile at the center.

The mold with reference 11937 is a blank mold, thus it has its own specificities such as having a lower capacity, simpler shapes and no engravings and two planes that define the region of interest in opposition to the ones previously mentioned. This mold was scanned with Scanner 3D CRONOS DUAL by Microsense for which there were no detailed specifications available.

Table 5.6: Results for real point clouds of Ref. 11937.

Ref.	11937
Real Volume (cm^3)	166,33
Computed Volume (cm^3)	160,35
Percentage Error	3,4%

The results for this mold are presented in Table 5.6 and for a manual selection of the planes that define the ROI. Since there was no unique criteria to automatically select these points, the operator must enter the two points in a graphical display of the center profile of the mold as in Figure 5.14.

This solution was then generalized for the molds mentioned previously as it is possible to observe in Figure 5.15.

56
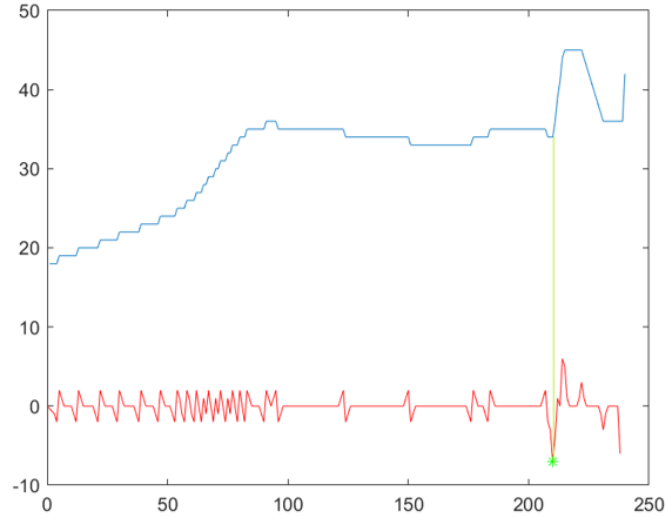
Figure 5.13: Automatic selection of the plane
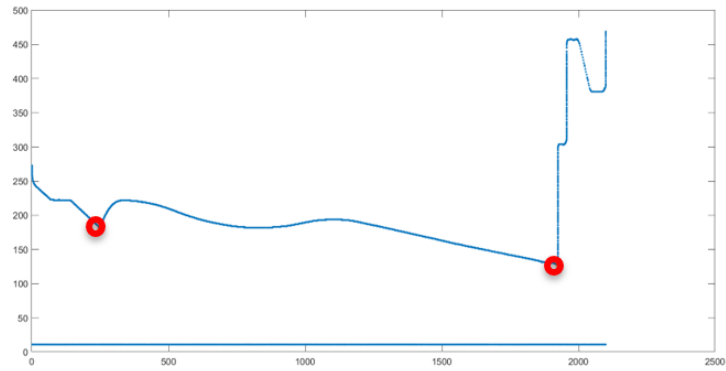
Figure 5.14: Manual selection of the planes for Ref. 11937

5.4.1 Simulation - Precision and Accuracy

One problem that arises is to confirm the accuracy and sensitivity of the model obtained.

As this method was implemented to address precision and accuracy it is necessary to test it for clouds with known volume that the method is actually working as intended.

In order to perform these tests a set of clouds was created with the method explained in Section 4.4

Accuracy

Table 5.7: Results for simulated point clouds without noise for volumes under 100 cm^3

Solid	Cylinder	Ellipsoid	Cube
Real Volume (cm^3)	58.9049	65.4498	64.0000
Computed Volume (cm^3)	58.8782	65.4739	64.3613
Percentage Error	0.0453%	0.0368%	0.5645%

These tests were repeated for the level of random noise in the range of the uncertainty of Einscan-Pro in Handheld Rapid Scan mode which is $\pm 0.3mm$.

(a) Ref. 0561　　　　　　　　(b) Ref. 2283

Figure 5.15: Manual Selection of the planes

Table 5.8: Results for simulated point clouds without noise for volumes above 330 cm^3

Solid	Cylinder	Ellipsoid	Cube
Real Volume (cm^3)	392.6991	366.5191	343.0000
Computed Volume (cm^3)	392.5794	366.5877	344.1068
Percentage Error	0.0305%	0.0187%	0.3200%

Table 5.9: Results for simulated point clouds of the solids in Table 5.7 with noise range [-0.3mm,0.3mm].

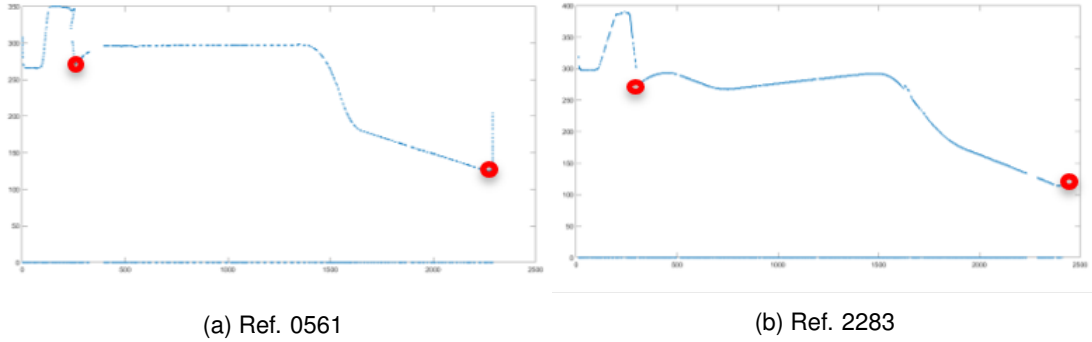| Solid	Cylinder	Ellipsoid	Cube
Real Volume (cm^3)	58.9049	65.4498	64.0000
Computed Volume (cm^3)	58.8782	65.4739	64.3613
Percentage Error	0.0453%	0.0368%	0.5645%

Table 5.10: Results for simulated point clouds of the solids in Table 5.8 with noise range [-0.3mm,0.3mm].

Solid	Cylinder	Ellipsoid	Cube
Real Volume (cm^3)	392.6991	366.5191	343.0000
Computed Volume (cm^3)	392.5794	366.5877	344.1068
Percentage Error	0.0305%	0.0187%	0.3200%

As it is observed, this level of noise does not affect volume measures, nevertheless it was taken into account that this range of uncertainty is for a single acquisition and one has also to account for the error in the fitting of the several acquisitions.

Precision

The tests show that the method has repeatability for the same data, and for that data with rotations and translation applied. This didn't happen with real data because of two factors: the limit number of iterations of ICP when fitting a top plane didn't always result in the same parameters since there is a random initial guess as a starting point. Also the selection of the ROI was performed manually introducing more uncertainty.

As these values of uncertainty are not precisely computed, the results are not presented since they would not represent a real tendency. Repeated tests were performed for the mold with ref. 2283 that allowed the usage of the automatic ROI selection showing a maximum variation of 0.5 cm^3.

Comparative test

A test with three molds of the same reference, produced in same series, molds number 8, 21 and 29 of the reference TN-483 produced by the Industrial Partner which corresponds to a 70cl bottle mold made of bronze. The scan of this reference was performed by Microsense.

The goals of this test are to compare the volumes between each mold and between the measures of the Industrial Partner, Microsense and CAD model.

Table 5.11: Results for the comparative test with three molds of the ref. TN-483

Mold number	test (cm^3)	Microsense (cm^3)	Manual (water filling) (cm^3)	Percentage Error (relative to Intermolde)
8	819.24	820.56	820.80	0.190%
21	820.86	821.44	821.80	0.114%
29	821.84	822.00	821.85	0.001%

5.5   Curvature detection - Existence and Precision

As stated by the Industrial Partner there is an apparent top plane in which molds' halves fit each other to close it, molds are designed to have a curvature of approximately 0.1% of the total longitudinal length.
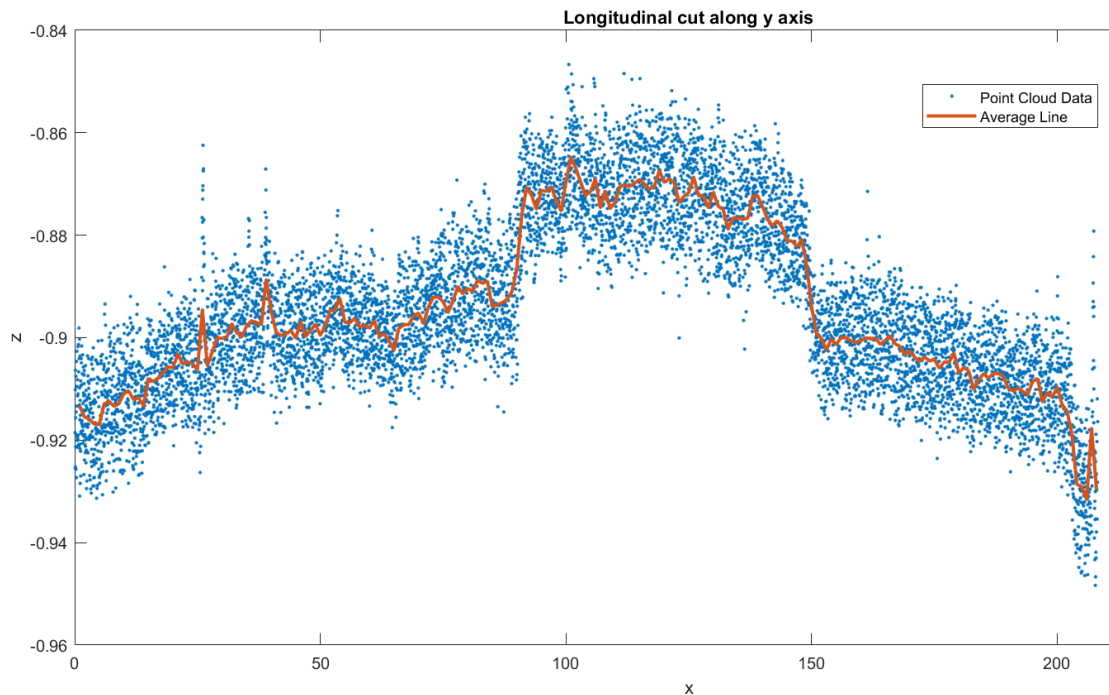
Figure 5.16: Longitudinal cut $21mm < y < 21.5mm$ showing curvature of the top of mold with Ref.11937, an average line is represented in red

For Ref. 11937 it was informed that for some molds the curvature is not designed to be perfectly concave, as it is the case of Ref. 11937, in particular for this reference there is a ramp in the first third of

the mold from -0.00mm to -0.15mm, a flat zone of constant -0.15mm and again in the last third a ramp from -0.15mm to +0.00mm.

It is possible to observe the result of the experience to detect the curvature of the vertical top of the mold in Figure 5.16.

Figure 5.16 shows the precision of the scanner, showing a variation of around 0.03mm for the same real position. This is caused, mainly, by the registrations of several point clouds into one. Although the shape present in the graph its not exactly as described one should consider that one is working at a scale below the accuracy of the scanner, thus it is not known for sure if the error exists in the mold or if it is caused by the scanning. Nevertheless the shape is detectable and possible to characterize through an average line.

This chapter has shown the result for the implemented methods and relevant tests that were performed. The next chapter presents conclusion withdrawn from the whole research.

Chapter 6

Conclusion

In the previous chapters the possibility of implementing a volume control measuring solution for the glass mold industry was studied. The need behind this research and the methodologies to follow were described. Several approaches were pursued and tested. The present chapter describes the conclusions withdrawn from the work developed.

The molds in scope are typically produced in bronze and cast iron, with complex features and engravings in the polished metal.

Several methods of data acquisition were used to acknowledge its advantages and disadvantages for the desired application. The ones considered the most promising and available were effectively tested in practice, performing a diversity of practical experiments in laboratory conditions.

Tests were carried out with IntelRealsense D415, Intel Realsense D435 and Kinect, cameras with no reconstruction algorithm relying in one acquisition only, that although showing promising results for applications of standard objects as boxes did not perform with sufficient precision and accuracy that would allow them to be considered for a mold volume measuring solution.

This cameras are designed to detect people or objects and its moves, meaning applications at a bigger scale. This devices have, for the purpose, low resolution, its perspective allows them to leave blind spots. This combined with bright surfaces cause the data to be incomplete. All this reasons motivated the search for a device closer to a metrological solution.

To obtain a higher level of precision and accuracy experiments were performed with visible light scanners from Shinning 3D, EinScan-SE and EinScan-Pro, in a price range considered low for industries but still around 6 times the price of the first cameras considered, as Intel Realsense.

As stated, the search was oriented to metrological devices, thus two more technological solutions were tested. Zscanner 700, a laser scanner and also a FARO Dual Cronos was used by Microsense, this last one was not taken into account when choosing a solution since little information about it was available.

Shinning 3D solutions have shown great potential in this application, not only because of its performance and price range but also by the fact that they are user safe. It is of great relevance to acknowledge that scanners in this price range usually require the use of sprays and powders to overcome polished surfaces reflection challenges. This problem is claimed to be solved in solutions from the same company especially designed for metrological applications, in a completely different price range, similar to the Zscanner 700 despite the fact that this one is still influenced by the bright surfaces.

In the development of an algorithm to compute volumes approaches proposed by other authors in different fields were critically discussed. This led to a first solution implemented, a simplification of the solution proposed in [1]. The simplification of this method led to the conclusion that the method would benefit from a better positioning of the camera. Nevertheless the results were consistent and the method

was able to approximate not only the box volume but also the 3 dimensions in detail.

The box solution was found to have several applications. Whether it is a matter of storage or transportation space optimization, the application is transverse to almost all the industries.

Methods such as ICP and RANSAC were studied as they played an important role in the algorithms proposed by other authors, although it was not implemented since Matlab already had a working and optimized function. In spite of this, basic tests to evaluate the results of the functions were carried out. Nevertheless RANSAC was not used.

The minimum squares criteria was widely explored and considered adequate to its application, and for that reason no other criteria was used for optimization.

Two solutions were developed and tested focusing on actual glass mold industry molds.

The Feature Recognition Approach was only tested in simulation and for a synthetic mold produced in the 3D printer. The time to return a result was below 20 seconds, way under the acceptable maximum time defined as 3 minutes. The maximum percentage error was defined as 10% and in practice it was always under 1%.

Although the results accomplished all the goals defined to the experiment the method is only adequate for simple shapes and it was intended to be applied to control large series as it requires specific developed for each mold design, as this is not the case in scope, this solution was not tested for real data.

In conclusion the Feature Recognition Approach is not suitable in practical terms for the main goal of measuring real data from molds.

A solution with the goal of being generalized for virtually every mold produced by the company was proposed, The Slicing Method. This solution was tested in simulation as well as with real data.

The simulation results were promising with the algorithm showing good precision and accuracy, as the percentage error was under 0.6%.

The biggest challenge dealing with real data from scanners was related with the approximation of the plane that should be considered for the volume measuring, referred to as the closing plane. As it is observable in 5.5 the closing plane is influenced with a relevant amount of noise that causes the plane to be defined differently at each acquisition for the same mold. This introduces a random bias in the results.

The approximation considered, and with the goal of generalizing a solution, did not take into account the concave regions of the molds, that can appear in both parts or just in one of them, depending on the client design.

The underlined idea was to consider a standard plane and then sum the extra volume created by this concave region as our concern was only the cavity. This issue also caused variability of the results since the considered plane was not placed in the standard position as ICP would reach the limit number of iterations before the desired plane was obtained. Also results variability was caused by the manual selection in some of the molds.

Different initial assumptions could benefit and improve the result's precision. Thus these issues will be further explored and suggested for Future Work in the next section.

In spite of the difficulties faced during the process, with limitations in hardware for not having a scanner dedicated to the project and in software as it was necessary to work only with software available with student access, satisfying results were achieved and most important a point was proven, that the solution has potential and it is crucial to learn from the limitations and invest in the project and further explore it, for that reason the next section defines guide lines for future development of this solution.

The industrial implementation problem persists and it will require automation and thus a repeatable protocol of image acquisition and processing has to be determined.

6.1 Future Work

The acquisitions were possible thanks to a group of professors and colleges that allocated some of their time and resources to this project. In future developments it is of great relevance that an appropriate scanner is allocated to the project allowing further tests.

It was acknowledged that for this type of industrial application the automation of the process of scanning with a robotic arm would benefit the solution as it would allow standardization of the data used in computation, it would overcome alignment issues as the robot itself by the end effector position would align point clouds instead of fitting them by an optimization process according to a criteria. This second method is not only less precise but it has higher probability of failing.

As referred before, it is left open for future investigation a solution that would overcome missing data challenges caused by shadows, dark surfaces and surfaces' reflectivity. It should be relevant to research the automatic closing of point clouds, even if several constraints should be assumed.

The first approach was related to the use of RGBD cameras. However due to the lack of required definition, the use of hand-held scanner was preferred. Attention should be paid to the developments in metal scanning technologies.

The industry remains searching for a practical solution that would aid or solve the quality inspection of its molds. The research techniques shown to be a feasible approach and a promising way forward to achieve this goal.

The problem still remains of great interest not only to mold producers but also to industries that order and use the molds as they desire to test the molds' wear and quality along time. Also the problem is extensible to several other industries that may see in this solution a way of optimizing its quality inspection and a way of assuring quality.

Bibliography

[1] B. Q. Ferreira, M. Griné, D. Gameiro, J. P. Costeira, and B. S. Santos, "VOLUMNECT: measuring volumes with Kinect," in *Three-Dimensional Image Processing, Measurement (3DIPM), and Applications* (A. M. Baskurt and R. Sitnik, eds.), vol. 9013, pp. 24 – 29, International Society for Optics and Photonics, SPIE, 2014.

[2] H. Mora, J. M. Mora-Pascual, A. García-García, and P. Martínez-González, "Computational analysis of distance operators for the iterative closest point algorithm," *PLOS ONE*, vol. 11, no. 10, pp. 1–19, 2016.

[3] MathWorks, "Matlab toolbox - ransac." `https://www.mathworks.com/help/vision/ref/ransac.html`. Accessed: 2019.

[4] P. Zanuttigh, G. Marin, C. D. Mutto, F. Dominio, L. Minto, and G. M. Cortelazzo, *Time-of-Flight and Structured Light Depth Cameras*. Springer, 2016.

[5] S. Giancola, M. Valenti, and R. Sala, *A Survey on 3D Cameras: Metrological Comparison of Time-of-Flight, Structured-Light and Active Stereoscopy Technologies*. Springer, 2018.

[6] "ISO 2859." `https://www.iso.org/sites/materials/standards-and-innovation/education_innovation-list.html`, 1989. Accessed: 2019.

[7] Intermolde, "Intermold's website." `https://we.tl/t-L4bGOHQp3m`, 2019. Accessed: 2019.

[8] X. Guo, F. Wang, Y. Ma, and D. Du, "Research on three-dimensional point clouds processing for standing tree volume based on laser scanner," in *2009 Second International Symposium on Knowledge Acquisition and Modeling*, vol. 3, pp. 206–208, 2009.

[9] Y. Lee and S.-Y. Cho, "A study on the waste volume calculation for efficient volume monitoring in a landfill facility," *The Journal of the Institute of Webcasting, Internet and Telecommunication*, vol. 12, pp. 153–159, 10 2012.

[10] H. T. Park, M. H. Chang, and S. C. Park, "A slicing algorithm of point cloud for rapid prototyping," in *Proceedings of the 2007 Summer Computer Simulation Conference*, SCSC '07, (San Diego, CA, USA), Society for Computer Simulation International, 2007.

[11] W.-C. Chang, C.-H. Wu, Y.-H. Tsai, and W.-Y. Chiu, "Object volume estimation based on 3d point cloud," in *2017 International Automatic Control Conference (CACS)*, pp. 1–5, IEEE, 2017.

[12] J. R. Rumble *Handbook of Chemistry and Physics*, 2019.

[13] Sonicam, "S3 Mold Gauging Machine Technical specifications." `https://sonicam.com/machines/mould-gauging-machine-s3/`. Accessed: 2019.

[14] MathWorks, "Matlab toolbox - icp." `https://www.mathworks.com/help/vision/`. Accessed: 2019.

[15] A. M. Wolfgang BOEHLER, "3D SCANNING INSTRUMENTS," 2007. i3mainz, Institute for Spatial Information and Surveying Technology, FH Mainz, University of Applied Sciences, Holzstrasse 36, 55116 Mainz, Germany.

[16] C. B. Norbert Pfeifer, "LASER SCANNING – PRINCIPLES AND APPLICATIONS," 2007. Vienna University of Technology Institute of Photogrammetry and Remote Sensing, Austria.

[17] D. Perreault, "3d scanning light sources: Red vs. blue vs. green." `https://3dscanningservices.net/blog/3d-scanning-light-sources-red-vs-blue-vs-green/`, 2017. Accessed: 2019.

[18] L. Hangzhou Shinning 3D tech co., "Einscan-pro quick start guide." `https://www.einscan.com/support/beginners-guide/`, 2017. Accessed: 2019.

[19] K. Otte, B. Kayser, S. Mansow-Model, J. Verrel, F. Paul, A. U. Brandt, and T. Schmitz-Hübsch, "Accuracy and reliability of the kinect version 2 for clinical measurement of motor function," *PLOS ONE*, vol. 11, pp. 1–17, 11 2016.

[20] J. Jiao, L. Yuan, W. Tang, Z. Deng, and Q. Wu, "A post-rectification approach of depth images of kinect v2 for 3d reconstruction of indoor scenes," *ISPRS International Journal of Geo-Information*, vol. 6, p. 349, 11 2017.